IMPACT OF BIOAEROSOL IN BUILDING MATERIALS AND ITS PREVENTION USING NANO SILICA COATING

A Thesis

Submitted for the partial fulfillment of the continuous assessment of M.Tech in Environmental Biotechnology course for the Session 2021-2023

By

JYOTI SAHA

Class Roll No. : 002130904009
Examination Roll No.: M4EBT23011
Registration No. : 160401 of 2021-2022

Under the Guidance of

DR. SUBARNA BHATTACHARYYA

Assistant Professor
Jadavpur University
(School of Environmental Studies)

SCHOOL OF ENVIRONMENTAL STUDIES

JADAVPUR UNIVERSITY

2023

It is hereby recommended that this **Thesis** entitled "***IMPACT OF BIOAEROSOL IN BUILDING MATERIALS AND ITS PREVENTION USING NANO SILICA COATING***" is prepared and submitted for the partial fulfilment of the continuous assessment of **Masters of Technology (M.Tech) in Environmental Biotechnology** course of Jadavpur University by **Jyoti Saha**, a student of the said course for the **session 2021-2023** under my supervision and guidance. It is also declared that no part of this thesis has been presented or published elsewhere.

…….

Dean
Faculty of Interdisciplinary Studies,
Law and Management (FISLM)
Jadavpur University

…….

Director
School of Environmental Studies
Jadavpur University

…….

Dr. Subarna Bhattacharyya

(Thesis Supervisor)

Assistant Professor
School of Environmental Studies
Jadavpur University

DECLARATION

This thesis entitled "IMPACT OF BIOAEROSOL IN BUILDING MATERIALS AND ITS PREVENTION USING NANO SILICA COATING" is prepared and submitted for the partial fulfillment of the requirements for the award of the degree of Masters of Technology (M.Tech.) in Environmental Biotechnology, course of School of Environmental Studies (Jadavpur University) for the session 2021-2023.

.....

JYOTI SAHA

Date :

School of Environmental Studies,

Jadavpur University.

CERTIFICATE OF APPROVAL

This is to certify that this thesis is hereby approved as an original work, conducted, and presented in a manner satisfactory to warrant its acceptance as a pre-requisite to the degree for which it has been submitted. It is implied that by this approval, the undersigned do not necessarily endorse or approve any statement made, opinion expressed or conclusion drawn therein, but approved for the purpose for which it is submitted.

Final Examination for valuation of Thesis

……

……

……

(Signature of the Examiner)

ACKNOWLEDGEMENT

This dissertation work had provided me the opportunity to meet and work with many people whose genuine cooperation and encouragement helped me to successfully complete my work on time. I would thus like to convey my sincere acknowledgement to all those, who in their humble ways had helped me enormously to complete my thesis.

Firstly, my deepest sense of gratitude and special thanks to my thesis supervisor **Dr. Subarna Bhattacharyya**, Assistant Professor, School of Environmental Studies, Jadavpur University, whose constant support, technical advice, and valuable guidance lead to the completion of thiswork. It was indeed an honor and a privilege for me to work under her supervision.

I would like to express my gratefulness to **Prof. Tushar Jash**, Director, School of Environmental Studies, Jadavpur University, to provide me the wonderful opportunity and facility to do this dissertation.

I would like to thank **Dr. Tarit Roychowdhury**, Associate Professor, School of Environmental Studies, Jadavpur University, for his continuous encouragement throughout my work.

I would like to convey my sincere gratitude to **Prof. Joydeep Mukherjee,** Professor, School of Environmental Studies, Jadavpur University, for his valuable suggestions and support during my dissertation.

I would also like to thank **Dr. Reshmi Das**, Assistant Professor, School of Environmental Studies, Jadavpur University, for her support and encouragement.

I would like to extend my sincere gratitude towards **Dr. Gagan Moi,** UGC-DAE, CSR, Kolkata centre for allowing and helping me analyze my samples using Micro EDXRF facility at his institute.

I would like to thank**, Prof. Dipak C. Pal**, Head of the Department, Department of Geological Sciences, Jadavpur University for allowing and helping me to use analyse my samples using Stereo Microscope facility at his department.

I would also like to thank **Mr. Samrat Sengupta**, laboratory in-charge/technician, Department of Civil Engineering, Jadavpur University, for allowing me to use his laboratory for the concrete cube preparation and to perform the mechanical tests on my samples.

I would like to show my gratefulness to **Dr. Goutam Pramanik** (facility in-charge), UGC-DAE,CSR, Kolkata centre for helping me in the FTIR analysis of my samples at his facility.

I would like to extend my deepest gratitude to my senior scholar **Anirban Chaudhuri,** whose continuous support, advices, and co-operation helped me exceptionally throughput my project.

My sincere thanks to all my senior scholars **Chiradeep Basu, Tanaya Bhowmick Goswami, Arup Roy, Shantanu Bhunia, Shayontani Basu, Iravati Ray, Kazi Hamidul Islam, Riashree Mondal.** Without their valuable help my dissertation would not have been a successful one.

I would like to express my appreciation to my fellow batchmates for their cooperation and encouragement.

I would also like to thank **The School of Environmental Studies**, Jadavpur University for giving me an opportunity to be a part of their family and providing me an excellent workspace.

Lastly, I would like to thank my parents and my siblings for always being my source of encouragement and confidence.

JYOTI SAHA

Kolkata, 2023

ABSTRACT

This study was aimed primarily to evaluate the impact of bioaerosol in building materials i.e. (Plain Cement Concrete and Fly Ash Concrete) and its prevention using nano silica coating.

The first part of the work dealt with the test tube analysis (preliminary study) which is done to evaluate which fungus is more dominant against deterioration of building materials by using small pieces of concrete cube, where we infected the pieces of Plain Cement Concrete and Fly Ash Concrete by *Aspergillus tamarii* and *Aspergillus niger* and kept the setup in incubator for 1 month at 27℃ for growth of fungus and after 1 month we carried the visual analysis i.e. colour changes, chemical analysis i.e. pH change in media, physical tests i.e. weight loss etc. which showed the result that *Aspergillus tamarii* is more dominant against biodeterioration of building materials than *Aspergillus niger.*

In the second part, concrete cubes of (Plain Cement Concrete and Fly Ash Concrete) (dimensions: 10 cm x 10 cm x 10 cm) were prepared and experimented in different set-ups namely control, biodeterioration (*Aspergillus tamarii* infected) and prevention (fungus infected nanocoated cubes). Analysis at intervals of 2 months and tests (visual, physical, and chemical) were done to evaluate the extension of the biodeterioration in the cubes, for six months. The visual analysis included colour changes, Stereo Microscopy and Scanning Electron Microscopy (SEM) which showed considerable change in the surface deterioration and fungal colonization of biodeteriorated cubes more than the nanocoated concrete cubes. The physical tests included weight loss whichshowed positive in all the concrete specimens and compressive strength which increased in nanocoated concrete cubes more than that of the biodeteriorated ones. The chemical analysis included pH change in media, Fourier Transform Infrared Spectroscopy (FTIR) and Energy Dispersive X-Ray Fluorescence Spectroscopy (EDXRF) which showed that leaching of calcium ions from the concrete in biodeteriorated cubes were higher than that of nanocoated cubes. Altogether the effectiveness of silicon oxide nanocoating against biodeterioration of *Aspergillus tamarii* was concluded to be positive.

Table of Contents

LIST OF TABLES

LIST OF FIGURES

CHAPTER I
INTRODUCTION

In Civil Engineering the most used material is concrete. Due to its strength, longevity, reflection, and versatility, concrete is a commonly used material in a variety of construction applications. Impact of bioaerosol is a global concern for biodeterioration of building materials. The issue of biodeterioration of the building materials has major impact on **economic aspects** along with other deterioration properties which results in the costly repair and maintenance. Many modern and historic stone structures around the world have been observed to experience biological deterioration and attack over time, which leads to an accelerated loss of their distinctive durable and aesthetic qualities. This has turned many heads for the various researches to investigate its causes to a great depth and to introduce feasible applicable techniques to prevent as well as restore these.

Deterioration is a phenomenon of degradation of materials to a lower vulnerable quality. When this deterioration is brought about by biological factors, it is termed as biodeterioration. Hueck (1965, 1968) described it as "any unfavourable change in a material's properties caused by the vital activities of organisms." It is normally perceived to be a negative process. A difference between ‘biodegradation’ and ‘biodeterioration’ has been put forward by Allsopp (2004) stating that when microorganisms modify materials with a positive or useful purpose it is referred to as ‘biodegradation’ and the negative impacts of a microbial activity is referred to as ‘biodeterioration.’

Bioaerosols are everywhere in the environment. The considerable financial burden of repair and maintenance makes concrete building deterioration a global concern. In addition to normal deterioration processes (cracking, erosion, corrosion of reinforcement, spalling, delamination etc.) concrete structures exposed to aquatic environments are prone to fouling by microorganisms (fungi) which not only affect their durability and integrity, but also the aesthetic appeal. The presence of various microorganisms on concrete is influenced by environmental conditions including temperature and humidity, as well as the properties and nature of the concrete surface like surface pH, initial porosity, and mineralogical nature of the substrate. Among different bioaerosols, fungi play more dangerous role in the bio-deterioration of building materials. The microorganisms form a biofilm over the surface of concrete and the metabolic activities of microorganisms leads to release of chemically aggressive ions that initiate the deterioration processes. Micro-organisms through their biological action

cause physical alteration to pore size, cracking, changes in water circulation, in the chemical composition of the surfaces that leads to weakening of the mineral structures. On concrete surfaces, a variety of fungi create pigments that cause discoloration and the development of dark staining patterns. Additionally, the surface of painted walls encourages the growth of fungi, leading to cosmetic issues and coating spalling.

Due to its increased siliceous and aluminous contents, which increase the durability qualities of concrete, fly ash is the most used cement substitute material. With regard to significant calcium leaching, low initial strength, strong carbonation, and low bacterial resistance, fly ash does have some disadvantages.

According to several research, adding nanoparticles of $CaCO_3$, TiO_2, etc. can significantly improve the characteristics of fly ash concrete. Additionally, it has been claimed that using inhibitors is a good idea if you want to reduce corrosion of the reinforcements embedded in concrete. In some cases, inhibitors based on sodium nitrite have also been found to have excellent antibacterial properties. The purpose of this study is to evaluate the fungal resistance of fly ash concrete after adding nano-modifiers and corrosion inhibitors. Microorganisms are prone to fouling concrete structures that are exposed to aquatic conditions, which not only compromises their longevity and integrity but also their aesthetic appeal.

The domain of potential biodeteriogens is quite extensive, starting from macroscopic organisms like fungi, moulds, algae, lichens, insects like termites, carpenter ants, wood boring beetles to microscopic beings like bacteria and cyanobacteria. Biodeterioration caused by bacteria, algae or fungi comprises a significant percentage, in cases of cultural heritage monuments. The severity and irreversibility of these deterioration are quite serious. Colonization of different microorganisms on historic buildings occurs gradually in a coordinated manner. It is mostly initiated by photolithotrophic algae and cyanobacteria having low nutrient requirements (sunlight, carbon dioxide and sufficient moisture). They secrete lactic, oxalic, succinic, pyruvic, and acetic acid thus degrading the stone substrate (Herera et al. 2004, Crispin and Gaylard, 2005).

Lichen at times develop on the concrete secreting organic acids releasing carbohydrates and amino acidspaved a path for the establishment of heterotrophs (bacteria and fungi). These heterotrophs penetrate the substrate producing organic acids (oxalic, fumaric, citric and 2-ketogluconic acids) and solubilizes the stone components consequently (Warscheid and Braams, 2000). This eventually worsens the physical surface of the substratum, allowing vegetal reproductive plant seeds to be deposited from air (cryptogams spores, weed seeds and higher plant seeds). This ecological succession gets completed when micro-fauna such as red mite *Balaustium murorum, Phaulioppia lucorum* inhabits the substratum (Tiano, 2002).

The mechanism of biodeterioration is influenced by the availability of nutrients and substrates, water permeability, mineral composition, pH, salinity and texture. Numerous environmental factors such as temperature, relative humidity (RH), and light conditions also influences the microorganism's growth on the substratum (Rajkwoska et al., 2013).

As multicellular, heterotrophic organisms, fungi are among the most well-known harmful microbes and are widely distributed in a variety of habitats (Biswas et al., 2013). They can be seen thriving naturally on various stone works andwooden structures and can effectively withstand dry conditions. The growth of black meristematic fungi which includes genera of *Alternaria, Aspergillus* and *Cladosporium* have resulted in surface erosion and micro-fractures in the Milan Cathedral of Italy (Capitelli et al., 2017). Genera like *Botrytis, Mucor* and *Trichoderma* produces citric andoxalic acid that solubilizes silicates and thus results in weathering of stones (Gorbushina et al., 2000). Water damaged and damp buildings are a breeding ground for moulds and fungus especially *Penicillium chrysogenum* and *Aspergillus versicolor* which are most common in water-damaged buildings, and *Chaetomium* spp., *Acremonium* spp., and *Ulocladium* spp being common in damp buildings (Andersen et al., 2011). The main focus for the study of biodeterioration of materials is the establishment of various prevention, control and restoration techniques against it. Ultra violet (UV) rays has a germicidal activity on algae, bacteria, and fungi with being highly effective duringtheir logarithmic phase of growth at low relative humidity (50%-60%).

Though its penetration power is low, it can modify the components such as proteins or cellulose of certain substrates (Tiano, 2002). Electromagnetic radiation such as gamma rays have been proved to be very much effective against moulds and insects developed on paper, parchment, and wood (Hickin, 1971). A biological agent such as the fungus *Scytalidium lignicola* can suppress the growth of *Lentinus lepideus*, which is a wood-decaying fungus.The former is commercially used and is hostile towards the growth of the latter biodeteriogen on archaeological wood (Bruce, 1998). Oxidizing agents like bromide, chloramine, ozone, aldehydes like formaldehyde, glutaraldehyde and esters of hydroxybenzoic acid (parabens) are all potential biocides. Isothiazolinones are also considered to be effective biocides. The methyl (MIT) and benzyl (BIT) derivatives are potent bacteriocides whereas the octyl (OIT) and the dichloro-octyl (DCOIT) derivatives show productive antialgal and antifungal activity (Allsopp, 2004).

Particles having dimensions within 1-100 nm range (nanoparticles) has unusual advantageous properties over their bulk counterparts. Thus, their use in the restoration process is a new inclusion. Titanium dioxide (TiO_2) nanoparticles are photocatalytic materials that can catalyze the complete degradation of many organic contaminants and has thus been used for protecting marble facades of historic buildings (Aldoasri et al., 2017). TiO_2 nanoparticles thus opposes degrading process due to biological attacks, stains or attacks by NOx and SOx. Silver (Ag) nanoparticles and titanium oxide (TiO_2) nanoparticles-based nanocomposite treatment of limestone in the Cathedral of Seville (Spain) showed effective biocidal effect (Becerra et al., 2018). Consolidates made from nanoparticles or nanocomposites of silicon (Si), titanium (Ti), silver (Ag), cadmium (Cd), iron (Fe), zinc (Zn) and cobalt (Co) have proved to be effective in the conservation of cultural heritage monuments and buildings (Fernandez et al., 2016).

Fungal attack on building materials especially concrete and their different prevention methods has been an interesting and ongoing topic for various research works in the last decade and has produced many convenient results. The incorporation of nanoparticles for better construction purposes and in admixtures, is probably a more recent addition to the numerous techniques developed for preventing microbial biodeterioration.

The data generated from the present study may prove helpful for the assessment of biodeterioration by common fungal species on concrete and its effective and non-destructive prevention using easily available nanoparticles.

CHAPTER II

AIMS & OBJECTIVES

The prime aim of this present dissertation work is to examine the impact of bioaerosol in building materials by *Aspergillus tamarii* and its effective prevention with the application of silicon oxide nanoparticles coating.

The study was carried out with the following objectives:

- To evaluate which fungal species is more harmful in deterioration of materials between (*Aspergillus tamarii* and *Aspergillus niger*).
- To evaluate the fungal biodeterioration effects on building materials like plain cement concrete and fly ash concrete caused by the infection of fungal species.
- To evaluate the effectiveness of the applied nanocoating with respect to the prevention of concrete biodeterioration by the infectionof fungal species.

Scope of study:

- ✓ Preliminary laboratory study (test tube analysis) of the proposed model on concrete pieces of plain cement concrete and fly ash concrete.
- ✓ Preparation of concrete cubes of dimension 10 cm x 10 cm x 10 cm for the biodeterioration and prevention tests.
- ✓ Assessment of the concrete specimens for six months at the interval of 2 months is carried out for physical, chemical and visual analysis i.e. pH of the media in which cubes were dipped for entire study, Colour Change Observation, Weight Loss Measurement, Compressive Strength Test, Stereo Microscopic Image, Micro Energy-dispersive X-ray fluorescence (Micro EDXRF) spectroscopy and Fourier Transform Infrared (FT-IR) spectroscopy analysis are done and evaluated.

CHAPTER III

LITERATURE REVIEW

3.1 Fungal Biodeterioration of Concrete: Review of Literature

Shelter is one of man's basic necessities, the dwelling place of a man i.e. buildings are thus needed to be protected from biodeterioration for the well-being of their own kind. On the other hand, heritage monuments and structures represent the roots of our culture and are too required to be preserved as well as restored from microbial attacks. Biodeterioration is thus a major cause in affecting buildings and monumental structures adversely.

One of the most commonly used material for construction purposes and being a $100 billion dollar industry, concrete is a structural material which is a composite of fine and coarse aggregates bonded together with the help of cement and water. The usage of concrete-like materials can be dated back to 6500 BC by the Nabataea traders or Bedouins inhabiting the Arabian Peninsula, North Africa, Iraq, and the Levant. It was also extensively used in the later Eras of Ancient Egyptians, Romans, and Greeks. Today, with time, the application and usage of concrete has drastically increased.

Concrete is made up of three major ingredients, aggregate that includes both fine and coarse materials like sand, gravel and crushed stones which helps in increasing the strength of the concrete, cement that is composed of alumina (2.5%-6%), silica (19%-23%), lime (61%-67%), iron (0%-6%) and gypsum (1.5%-4.5%) and water that allows the cement to move freely (slurry like).Cement hardens when mixed with water and binds all the ingredients together. Portland cement is the most widely used cement at present times. Stronger, more durable concrete should have a lower water-to-cement ratio. The property of the final product depends on the ratio of these ingredients. Admixtures are often added to adjust the concrete mixture for specific performance. Strength, durability, versatility, and affordability are the properties that makes concrete the most preferable building material.

Through the biochemical processes that the microbial species uses to respond, develop, and multiply, building materials, especially concrete, are susceptible to severe physical, chemical, mineralogical, and microstructural irreversible damages (Bertron 2015).

Fungus has a capability to do so with their developing hyphae that etches and into the interior of the concrete. This was proved by the study done by Gu et al., (1998) showing that with the fungal proliferation of Fusarium on concrete for 120 days, organic acids were excreted that resulted in the dissolution of the available calcium and magnesium ions in the concrete. Dissolution of these ions lowered the pH of concrete which resulted in an unstable state of the binding paste and hence gets more prone to mechanical weathering (Mehta et al., 1999) and cracks can easily develop in them (Gu et al., 1998). This adversely affected the porosity of the concrete by increasing it and enlarging the damaged area. Because of this the weight and compressive strength of the concrete also got affected (Gu et al., 1998).

A study conducted by Biswas et al., 2012 stated that pre-historic caves in Kabra-Pahad (Chattisgarh) were found to have undergone destructive microbial deterioration. When the microbe organisms were isolated from the affected regions of the natural structure, it was found that Aspergiilis sp. was the most predominant one among all the other isolated species.

Biogenic weathering effects of fungal species: Aspergillus niger, Serpula himantioides and Trametes versicolor on apatite, galena and obsidian minerals by Adeyemi et al.,(2005) using EDXRF and SEM micrographs showed that the interactions of metabolites like H+ and organic acids exuded by these fungus were the primary responsible force for the modification of the mineral substrates of the rocks into the transformation of secondary minerals or crystals and subsequently leading to the corrosion of the mineral surface.

According to Wei et al. (2013), corrosion in concrete sewer lines and structures is a major issue around the world as a result of microbial colonisation, succession, and its induced deterioration through the formation of organic and inorganic acids.

3.2 Prevention of Fungal attack using Silicon oxide Nanoparticles: Review of Literature

Nanotechnology is the newest trend of most of the scientific researches and developments that are taking place in this century. Nano-sized particles exists at near atomic levels and can be enhanced to cater mankind's needs appropriately.

Silicon dioxide is the main component of beach sand as silica being the second most abundant element found on Earth's surface. Silicon dioxide nanoparticles (also called silica nanoparticles or nanosilica) have properties of stability and ability to be functionalized with a wide range of molecules and polymers. The P-type nanosilica particles have higher surface area than S-type nanosilica particles, having a pore rate of 0.061 ml/g and flaunts higher ultraviolet reflectivity. Commercially available SiO_2 NPs with average particle size of 7 -14 nm and a specific surface area of 100-150 m2/g exhibits prominent hydrophobicity.

Alcohol suspension of SiO_2 NPs when sprayed onto a paper by Ogihara et al., (2012*),* formed a transparent coating and imparted super hydrophobicity to the paper. The hydrophobic character of SiO_2 NPs can be enhanced by the incorporation of hybrid siloxanes or silicone polymers which presented a high-water repellant capacity generating superhydrophobicity. Superhydrophobic surfaces displays a wetting characteristic witha very high static contact angles (water contact angle with the surface) which can be greater than 150°. Mixing alkoxysilane and silica nanoparticles synthesized by sol-gel route using HCl as a catalyst and ethanol as a solvent, De Ferri et al.(2011) obtained a superhydrophobic product for stonework.

Studies conducted by Falchi et al.(2013) showed that application of commercial nanosilica with an average radius of 9-55 nm, on limestone (Lecce stone) has proved to be a strong consolidant. The pre-treatment of the surface with ethanol and the nanoscale size of the silica particles resulted for a better consolidation action. Surfactant-synthesized silicon-based hybrid nanocomposites such as tetraethoxysilane (TEOS) and methyltrimethoxysilane (MTMOS) are among the most widely used stone consolidants due to their ability to penetrate easily into porous matrix (Wheeler et al. 2005). The addition of small amount of surfactant like n-octylamine during the nanocomposite preparation gives crack-free consolidants for stone conservation (Mosquera et al., 2012). These silica-based consolidants can hence be considered fairly compatible with silicate stones.

SiO_2 NPs expresses good inhibitory property of different bacterial strains. Their smaller size and higher surface to volume ratio enables them to bind with the microbial strains and thus contributed to their antimicrobial potential. A study by Farrukh et al.(2016) showed that ZnO-SiO_2 nanocomposite exhibited antibacterial activity against *Bacillus subtilis* (gram positive) and *Escherichia coli* (gram negative) strains and antifungal activity against *Candida parapsilosis* and *Aspergillus niger*. SiO_2 in the nanocomposite was also observed to enhance the photo-catalytic activity of the nanocomposite.

In another research conducted by Scevola et al.,(2012*)* a product named SIAB was synthesized which consisted of stable nanosilica functionalized with ionic Silver. The antimicrobial property of SiO_2 NPs was observed to be improved by the covalent bonding of the Ag ions, stabilized in their one electron oxidized form. The activity of SIAB was tested against various gram-positive and gram-negative bacteria and fungi. *Staphylococcus aureus*, *Enterococcus* spp., *Streptococcus pyogenes*, *Streptococcus salivarius*, *Streptococcus mitis*, *Pseudomonas aeruginosa*, *Escherichia coli* and *Candida albicans*. It was concluded from the study that SIAB showed high bacterial and high fungicidal action against these strains.

The replacement of cement with nanosilica having an average particle size of 15 nm and 80 nm showed an increase in compressive strength of the nanosilica blended concrete. An increase in flexural and split tensile strength as well was observed in blended concrete with 80 nm nanosilica (Givi et al., 2010).

In another study conducted by Li et al., (2004) showed that nano Fe_2O_3 and nano silica mortars exhibited higher 7 days and 28 days compressive strength than normal concrete. The analysis of the microstructure showed that due to pozzolanic reaction, nanoparticles filled up the pores and substituted the reduced calcium hydroxide amount.

The incorporation of nanosilica can improve the microstructure to be more uniform and compact as compared to normal concrete thus enhancing the resistivity of concrete to water (Ji, 2005).

CHAPTER IV

METHODOLOGY

4.1 Preparation of Fungal Spore Suspension:

4.1.1 Pure Culture Preparation:

Pure culture of *Aspergillus tamarii* and *Aspergillus niger* were prepared in Czapek Dox agar slants initially. 50 ml of Czapek Dox media was prepared in eight 100 ml conical flasks as per the following Czapek Dox Composition: (HiMedia Technical Data).

Ingredients	**Amount (gms/litre)**
Sucrose	30
Sodium nitrate	2
Dipotassium phosphate	1
Magnesium sulphate	0.5
Potassium chloride	0.5
Ferrous sulphate	0.01
Agar	15
Final pH (at 25°C)	7.3±2

The ingredients were mixed, pH was adjusted, after adding the agar the media was autoclaved at 121°C temperature at 15 pounds per square inch (1.0546 Kg/cm^2) pressure for 30 minutes. 100 ml of distilled water was also autoclaved for control. After the sterilization of Czapek Dox media, it was cooled and kept at an angle of 45° overnight for solidifying, at room temperature. After solidification, the agar slants were streaked with a loopful (inoculating loop) of pure culture of *Aspergillus tamarii* and *Aspergillus niger* and then incubated at their optimum growth temperature of 27°C for 7 days.

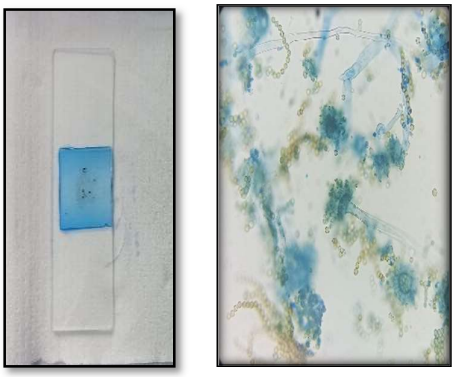

Figure 1: Microscopic view of *Aspergillus tamarii*

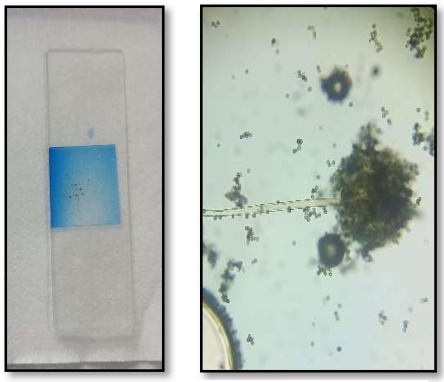

Figure 2: Microscopic view of *Aspergillus niger*

Figure 3: (A) Autoclave (B) 100 ml conical flask with autoclave distilled water (C) CZAPEK Dox Media

Figure 4: Slant Preparation

Figure 5: Incubator

Figure 6: Slant having growth of *Aspergillus tamarii*

Figure 7: Slant having growth of *Aspergillus niger*

4.1.2 Spore Suspension Preparation:

On completing the incubation period of 7 days, the slants were taken out of the incubator and 50 ml of autoclaved (sterile) distilled water was added to each flask. The flasks were shaken properly so that the spores from the pure culture gets suspended into the added sterile distilled water. The total 100 ml of spore suspension (50 ml from each of the 2 flasks i.e. 1 for *Aspergillus tamarii* (50ml) and 1 for *Aspergillus niger* (50ml) was thus collected in a fresh autoclaved conical flask and was stored for further use.

Figure 8: Spore Suspension of *Aspergillus niger*

Figure 9: Spore Suspension of *Aspergillus tamarii*

4.2 Nanoparticle Coating Preparation:

Silicon oxide nanoparticles were commercially obtained (Platonic Nanotech Private Limited) having the following specifications:

Chemical Formula	**:**	SiO_2
Physical Form	**:**	Powder
Colour	**:**	White
Purity	**:**	99.55%
Average Particle Size	**:**	30-50 nm
Specific Surface Area	**:**	200-250 m^2/g
Atomic Weight	**:**	231.533 g/mol
Bulk Density	**:**	0.10 g/cm^3
True Density	**:**	2.5 g/cm^3
Morphology	**:**	Porous
Molar Mass	**:**	60.08 g/mol
Melting Point	**:**	1600 °C

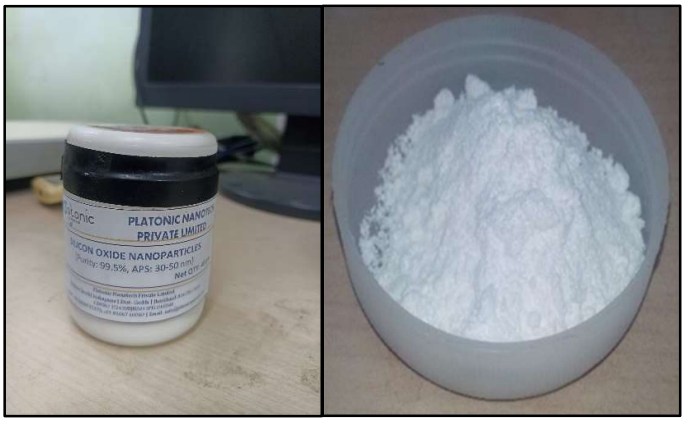

Figure 10: Silicon oxide nanoparticles

4.2.1 Binder Preparation:

Polyethylene glycol (PEG) was dissolved in ethanol [1:1 ratio] by gently heating in a water bath at 35°C for 20 minutes.The PEG flakes dissolved to give a thick, translucent, and viscous solution.

Figure 11: Polyethylene glycol and Alcohol

Figure 12: A thick, translucent, and viscous solution.

4.2.2 Preparation of Nanoparticle Coating:

Combination of binder, silicon oxide nano-powder and water (1 : 0.5 : 2) was chosen to be proceeded further in the study. The optimization of the ratio of the nanoparticle coating was done by Bhattacharyya et al. (2022).

Figure 13: Combination of binder, silicon oxide nano-powder and water (Nano Silica Coating)

For the study; 14 ml binder, 7 g Silicon oxide nanopowder and 28 ml distilled water were mixed and sonicated for 5 minutes (avoiding froth formation on the surface) at room temperature. A milky white homogenous solution of nanoparticle coating was obtained.

4.3 Preliminary Laboratory Study: (Test Tube Study)

4.3.1 Fungal Biodeterioration of Plain Cement Concrete and Fly ash Concrete Pieces (First month study):

24 concrete pieces i.e., 12 pieces of Plain Cement Concrete and 12 pieces of Fly ash Concrete were hammered to approximately same size and their initial weights were measured. 250 ml of Czapek Dox media was prepared and autoclaved. The media was then cooled down to room temperature. 24 No's of Test tube is properly washed and rinsed with water and labelled, in each test tube 10ml of above prepared medium is poured with help of funnel and measuring cylinder. 1 ml of fungal spore suspension of *Aspergillus tamarii* and *Aspergillus niger* was added to the test tubes that were marked for biodeterioration study of the concrete pieces (spore suspension to media ratio being (1:10)).

Figure 14: Plain Cement Concrete Pieces

Figure 15: Fly Ash Concrete Pieces

Figure 16: Test Tube containing CZAPEK Dox Media

Figure 17: Test Tube containing CZAPEK Dox Media and Concrete Pieces

Table 1: Test Tube Setup

FLY ASH CONCRETE (12 Test Tube Required)	**PLAIN CEMENT CONCRETE (12 Test Tube Required)**
For *Aspergillus tamarii*	**For *Aspergillus tamarii***
3 No. of Test Tube-Control (Without infection)	3 No. of Test Tube-Control (Without infection)
3 No. of Test Tube-Infected (With *Aspergillus tamarii*)	3 No. of Test Tube-Infected (With *Aspergillus tamarii*)
For *Aspergillus niger*	**For *Aspergillus niger***
3 No. of Test Tube-Control (Without infection)	3 No. of Test Tube-Control (Without infection)
3 No. of Test Tube-Infected (With *Aspergillus niger*)	3 No. of Test Tube-Infected (With *Aspergillus niger*)

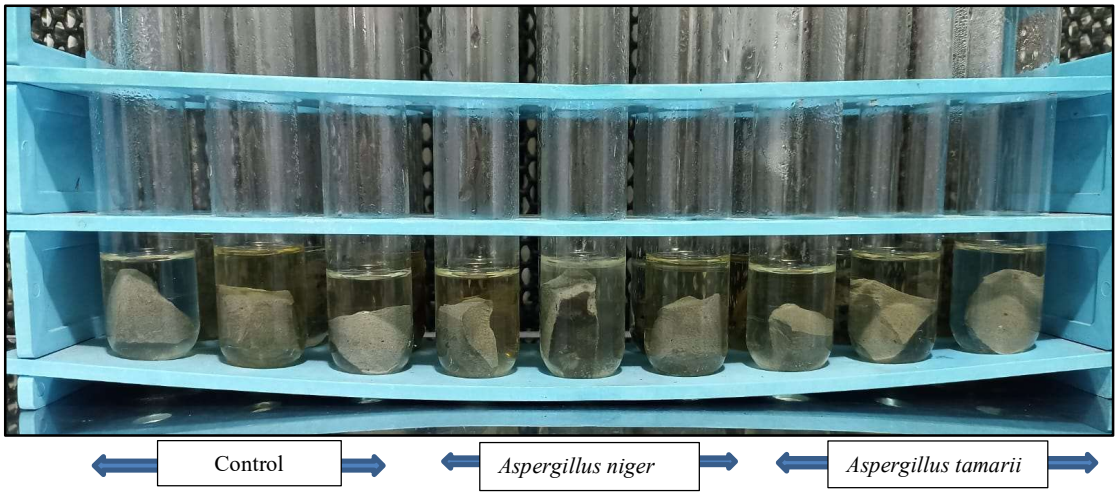

Figure 18: Fly Ash Concrete pieces infected with *Aspergillus niger* and *Aspergillus tamarii*

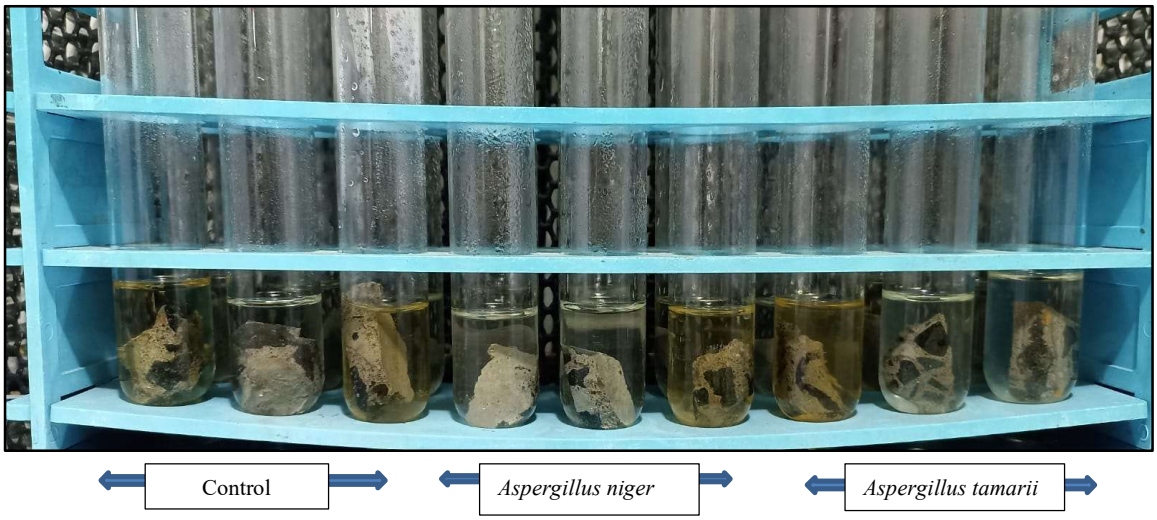

Figure 19: Plain Cement Concrete pieces infected with *Aspergillus niger* and *Aspergillus tamarii*

The test tubes were cotton plugged, the control setup was kept at room temperature and the biodeterioration setup was placed in the incubator at 27°C for 1 months. At the end 1 month, the test tubes was removed from incubator, concrete pieces were washed and air dried to record the colour change and the weight loss percentage of the respective concrete pieces and pH of the media were measured after 1 month.

4.4 Study of Fungal Biodeterioration and its Prevention using Nano silica particle coating:

4.4.1 Preparation and making of Concrete cubes:

Concrete cubes of standard grade M25 (final compressive strength after 28 days of curing: 25 Mpa or 25 N/mm^2) were made as follows:

As per design standard of grade M25, cement, sand (fine aggregate) and stone chips (coarse aggregate) were weighed according to the ratio of (1:1:2). Firstly, the sand and cement were mixed thoroughly in dry condition using a shovel to achieve a uniform colour. Then the stone chips were added and the entire batch were mixed uniformly. Water was then added to this mixture (water to cement ratio being 0.5) and all the components were homogenously mixed to obtain the desired consistency.

Cubic cast iron moulds were cleaned and oiled and the freshly mixed concrete was then immediately filled up in the moulds, layer by layer, followed by uniform compaction using a compacting bar to eliminate any void. The moulds were filled and the top surface was leveled by a trawler. The moulds were then kept at room temperature for24 hours.

After 24 hours, the moulds were removed and solid concrete cubes of dimension 10 cm x10 cm x 10 cm were obtained. These cubes were then submerged in clean water for 28 days for curing. Having gained the maximum strength, the cubes were taken out of water and dried for 3 days at room temperature. The initial weights of the cubes were recorded in aweight balance followed by the measurement of their initial compressive strength.

Casting of Plain Cement Concrete Cubes (10cm x 10cm x 10cm)

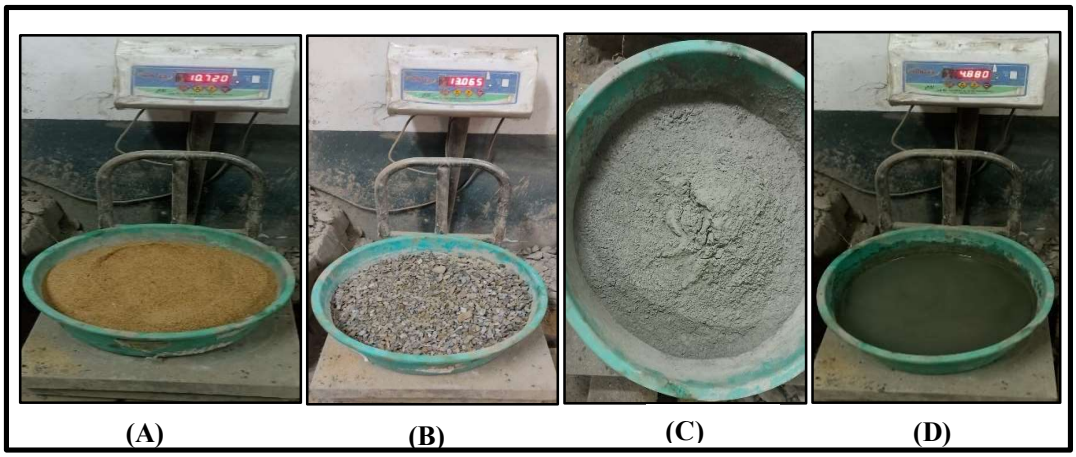

Figure 20: Casting of Plain Cement Concrete Cubes (A) Sand (B) Stone Chips (C) Cement (D) Water

Figure 21: Mixture of above ingredients

Figure 22: Casting Moulds

Figure 23: Mixture compacted in the moulds

Figure 24: After 1 day of air drying

Figure 25: Curing done for 28 days under water

Casting of Fly ash Concrete Cubes (10cm x 10cm x 10cm)

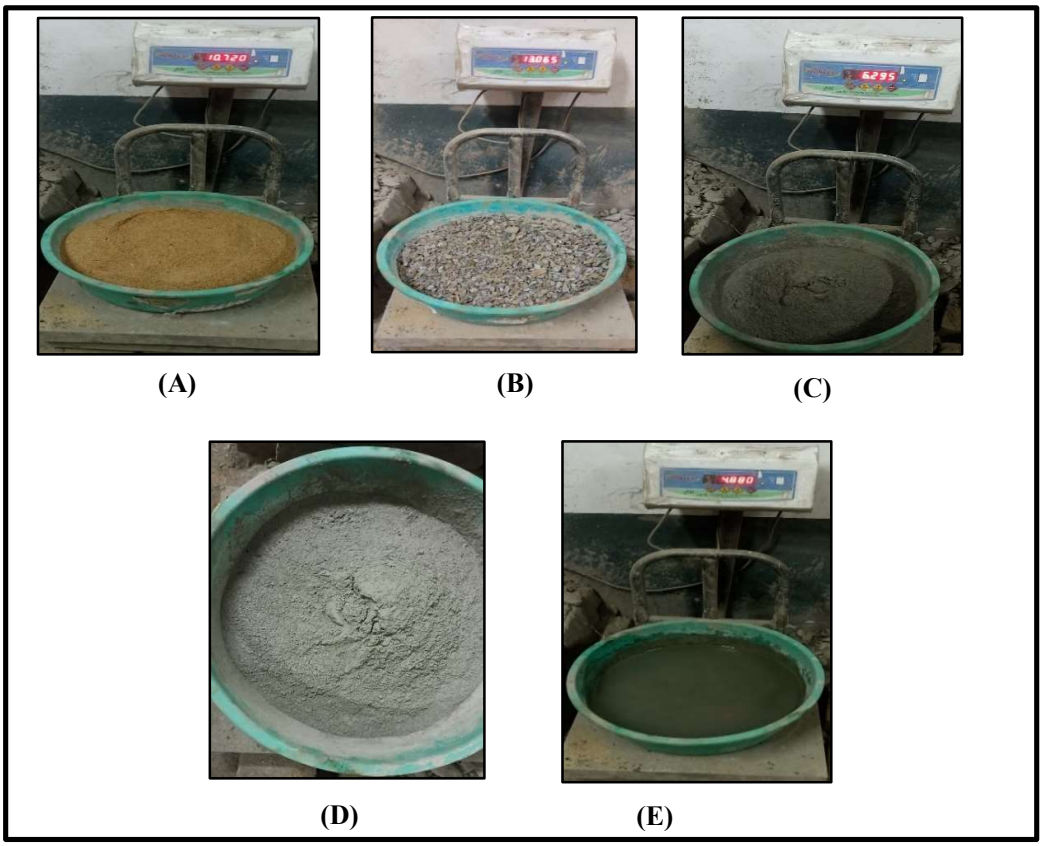

Figure 26: Casting of Fly ash Concrete Cubes (A) Sand (B) Stone Chips (C) Fly Ash (D) Cement (E) Water

Figure 27: Mixture of above ingredients

Figure 28: Mixture compacted in moulds

Figure 29: Curing for 28 days under water

4.4.2 Nanocoating the cubes:

The fly ash concrete cubes that were selected for the study of prevention of fungal biodeterioration were brushed uniformly with the previously prepared Silicon oxide nanocoating. These cubeswere then kept in the hot oven dryer at 40°C and were dried for 4 days.

Figure 30: Nano Silica Coating

Figure 31: Applying nano silica coating in concrete surface

Figure 32: Drying the coated cubes in hot air oven

4.4.3 Media Preparation:

15 L of Czapek dox Media was prepared. It was mixed properly with the help of a magnetic strier. It was then autoclaved for 40 minutes and cooled down to room temperature.

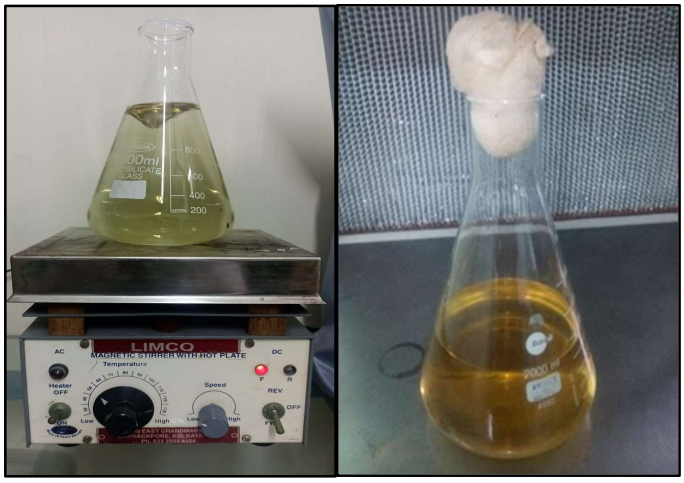

Figure 33: CZAPEK Dox Media Preparation

4.4.4 Preparing the experimental setups:

Polyethylene boxes were washed in tap water and further the surface of the boxes were sterilized with ethanol followed by UV radiation treatment for 1 hour and the boxes were marked to study the biodeterioration and the prevention process, along withthe addition of 2 L of Czapek Dox media and 200 ml of fungal spore suspension (we will take the fungal spore suspension of that fungus which will show more dominant against deterioration of building materials between *Aspergillus tamarii* and *Aspergillus niger* from the above preliminary test tube study result) to each of these boxes. The cubes were distributed in all the boxes and were tightly sealed and marked properly.

The arrangement was as follows:

Set-up		**Contents**
Control	➞	Box + Czapek Dox media + Concrete cubes
Biodeterioration	➞	Box + Czapek Dox media + Fungal inoculation + Concrete cubes
Prevention	➞	Box + Czapek Dox media + Fungal inoculation + Nanocoated Concrete cubes

This experimental setup was kept at room temperature for 6 months and after every 2 months interval the cubes from each set were removed and tested to observe the changes And respective data were recorded and analysis were done.

Figure 34: Experimental Setup arrangement

4.5 Tests and Analysis done on the Concrete cubes:

4.5.1 Humidity measurement:

For six months the humidity inside the boxes containing Plain Cement Concrete and Fly ash Concrete Cubes were recorded at the interval of two months using a digital humidity meter for control, biodeterioration and prevention setup.

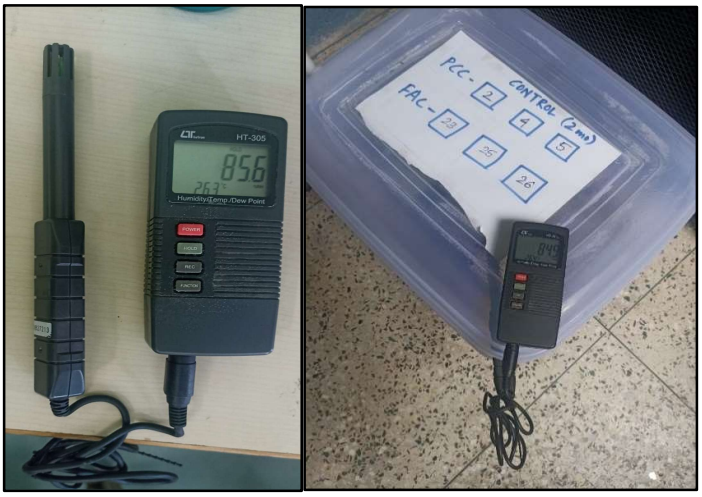

Figure 35: Digital Humidity meter (Lutron)

4.5.2 pH measurement:

For six months at the interval of two months, the pH of the media at the bottom of the boxes containing Plain Cement Concrete and Fly ash Concrete Cubes in control setup, biodeterioration set-up and the prevention set-up, contained in the boxes, were checked, and noted down using a digital pH meter.

4.5.3 Colour change observation:

For six months at the interval of two months, concrete cubes (plain cement concrete and fly ash concrete cubes) from each of the experimental set-up (3 cubes each from control, biodeterioration and prevention set-ups respectively) were taken out, thoroughly cleaned, and then dried in hot air oven for 4 hours at a temperature of 50±5 °C.

The concrete cubes (plain cement concrete and fly ash concrete cubes) were then observed by naked eye and simultaneously compared to a geological rock colour chart (Munsell, 2003), for any colour change.

4.5.4 Weight loss measurement:

After the concrete cubes were prepared and dried properly, initial weights of each concrete cube (plain cement concrete and fly ash concrete cubes) were measured in a weighing machine. The cleaned, dried and desiccated concrete cubes taken out at the interval of two months from the respective experimental set-ups, were weighed in the weighing balance to record their final weights of plain cement concrete and fly ash concrete cubes.

Figure 36: The weight of a concrete cube is being measured in the weight balance.

From the weights measured, the percentage weight loss of the concrete cubes was calculated using the formula:

$$\text{Change in weight (kg)} = (W_1 - W_2) / W_1$$

Where, W_1 = Initial weight of the concrete cube (kg)

W_2 = Final weight of the concrete cube (kg)

So, Percentage weight loss (%) = change in weight x 100

4.5.5 Stereo Microscope:

A stereo-microscope is an optical microscope having a low magnification with a longer working distance. It primarily uses two separate optical paths using two separate objectives and eye pieces for each eye thus yielding a three-dimensional visualization of the specimen. It also uses reflected illumination of the specimen i.e. it utilizes the light that is naturally reflected from the object rather than transmitted through it. These features altogether make it ideal for examining solid material's surfaces, circuit board inspection, watch making and to be used in dissection, microsurgery, and in forensic engineering.

Figure 37: Stereo Microscope

Figure 38: Concrete cube observed under the stereo microscope.

The concrete cubes (plain cement concrete and fly ash concrete cubes) that were taken out from all the set-ups (for 6 months at 2 months interval) were observed under the stereo microscope to note any change on their infected surface.

4.5.6 Compressive Strength test :

Compressive strength is the maximum stress that a solid material can sustain without fracture, under a gradually applied load tending to reduce size. Determining the compressive strength of concrete is the most common performance measurement and a key value for designing structures.

The compressive strength of the cubes was determined using a Universal Compressive Strength Test Machine. Each concrete cube specimen was placed between the platen such that the load could be applied on opposite sides of the cubes, and the axis of the specimen and the center of thrust of the spherically seated platen are vertically aligned. Load was applied to the specimen at an increasing rate of 140 kg/cm^3 per minute till the specimen collapsed. The peak load or the maximum applied load at which the cube failed was noted and the corresponding compressive strength was calculated as follows:

$$\text{Compressive Strength of Concrete (N/mm}^2\text{)} = \frac{\text{Maximum Load applied to the cube}}{\text{Cross–Sectional Area of the cube}}$$

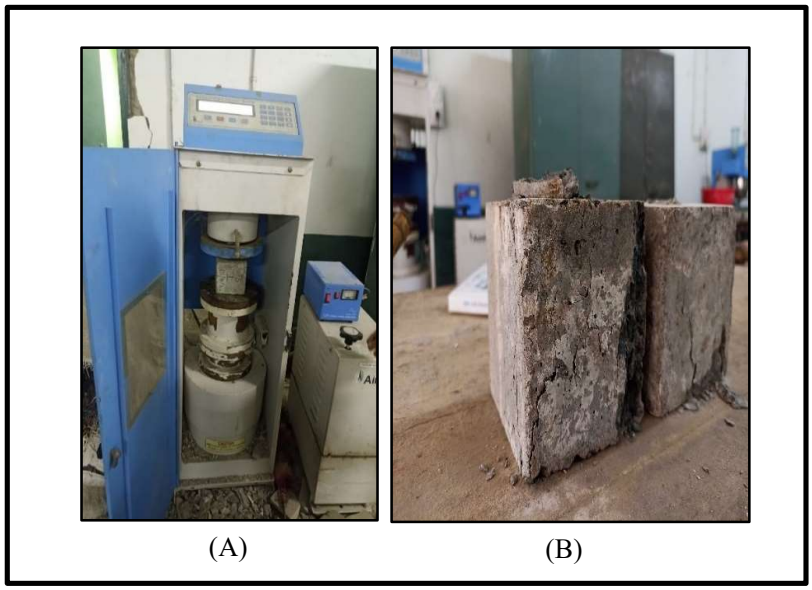

Figure 39: (A) Universal Compressive Testing Machine (B) Collapsed and broken cube

During the compressive strength test, all the concrete cubes (plain cement concrete and fly ash concrete cubes) were found to be collapsed and broken under compressive load. Small pieces of concrete cubes were then collected from these broken cubes to be further tested and analyzed in various other sophisticated instruments.

4.5.7 Fourier Transform Infrared Spectroscopy (FT-IR):

Fourier Transform Infrared Spectroscopy is an analytical technique that identifies the organic, polymeric, and sometimes inorganic components of a sample using infrared absorption or emission of the solid, liquid or gaseous sample, over a wide spectral range. The basic principle of FT-IR is by shining a beam of light, containing many frequencies, on the sample resulting in the production of an interferogram of sample signals. The FT-IR then collects these interferogram of signals using an interferometer, digitizes and performs a Fourier Transform (FT) function on the interferogram and displays the spectrum.

Spectral quality determination is an important step in the spectrum interpretation process. General classification of materials by its major functional groups can be done with a good quality spectrum whereas a poor-quality spectrum can misrepresent the true absorption band positions, shapes, and intensities.

One of the popular interpretations of the resultant spectra is through spectral fingerprinting where the spectrum of the unknown sample is compared to the known molecular configurations, in order to determine the structure of the unknown sample. The spectrum is divided into several frequency regions and the presence or absence of absorption bandsin each region interprets the sample characteristics.

Figure 40: Fourier Transform Infrared Spectrometer (FT-IR) Frontier.

The small pieces of concrete cubes (plain cement concrete and fly ash concrete cubes) that were earlier collected after the compressive strength test, were uniformly crushed using a mortar and a pestle, and the corresponding homogenous powder of concrete was used in FT-IR spectroscopy analysis.

Figure 41: Small pieces of concrete cubes collected after compressive test

Figure 42: Mortar and pestle

Figure 43: Crushed powdered sample

Figure 44: KBr pellet

4.5.8 Energy Dispersive X-Ray Fluorescence Spectroscopy (EDXRF):

Energy Dispersive X-Ray Fluorescence spectroscopy (Horiba Scientific, XGT-7200) is a highly accurate, non- destructive technique for the elemental analysis (both qualitative and quantitative) of anunknown sample. The complete breakdown of the composition to elemental level, of known as well as unknown materials in terms of percentages or ppm (parts per million) is easily obtainable. In EDXRF spectrometers, concurrent excitation of all the elements in a sample are done which emits a fluorescence radiation. This fluorescence radiation from the sample is collected using an energy dispersive detector along with a multi- channel analyzer which simultaneously separate the different energies of thecharacteristic radiation from each of the different constituent elements of the sample.

Figure 45: Energy Dispersive X-Ray Fluorescence (EDXRF) Spectrometer

The chips size samples of concrete, obtained from crushing of the small concrete pieces were collected, and were analysed in the EDXRF spectrometer.

Figure 46: Chips size samples of concrete

CHAPTER V

RESULTS & DISCUSSIONS

5.1 Preliminary laboratory study:

5.1.1 Fungal Biodeterioration of Concrete Pieces (First 1 month test tube study) :

5.1.1.1 Colour change Observation:

a) **Initial colour :**

b) **Control :**

c) ***Aspergillus niger* infected pieces :**

d) ***Aspergillus tamarii* infected pieces :**

Figure 47: Observed colour changes with their colour codes (as per Geological Rock Colour Chart-Munsell, 2009)

a) **Initial Colour- Pinkish gray (5YR 8/1)**
b) **Control- Pinkish gray (5YR 8/1)**
c) **Biodeterioration after 1 months (*Aspergillus niger*)- Yellowish gray (5Y 8/1)**
d) **Biodeterioration after 1 months (*Aspergillus tamarii*)- Yellowish gray (5Y 8/1)**

It was observed that the concrete pieces of the biodeterioration set-up over the time lost its original colour (as could be seen in control) and after infection with fungus it became more paler and rustier in case of *Aspergillus tamarii* than *Aspergillus niger*.

5.1.1.2 Weight Loss Percentage (%):

CONCRETE MATERIAL - FLY ASH CONCRETE INFECTED WITH *Aspergillus niger*

Table 2: Weight Loss Percentage of fly ash concrete pieces of control over 1 month.

Test Tube Setup	Weight (g)		Weight Loss (g)	Weight Loss Percentage (%)	Average Weight Loss Percentage (%)
	Initial	Final			
Control	3.243	3.317	0.074	2.281	1.7733±0.442
	6.054	6.143	0.089	1.470	
	2.232	2.267	0.035	1.568	
Infected With *Aspergillus niger*	2.260	2.108	0.152	2.725	2.377±0.311
	4.848	4.745	0.103	2.124	
	5.081	4.965	0.116	2.283	

CONCRETE MATERIAL - FLY ASH CONCRETE INFECTED WITH *Aspergillus tamarii*

Table 3: Weight Loss Percentage of fly ash concrete pieces of biodeterioration over 1 month.

Test Tube Setup	Weight (g)		Weight Loss (g)	Weight Loss Percentage (%)	Average Weight Loss Percentage (%)
	Initial	Final			
Control	3.757	3.838	0.081	3.183	3.358±0.281
	4.236	4.331	0.095	2.849	
	3.783	3.874	0.015	3.409	
Infected With *Aspergillus tamarii*	2.857	2.730	0.127	2.345	2.637±0.250
	2.596	2.432	0.164	2.711	
	2.216	2.093	0.123	2.825	

CONCRETE MATERIAL – PLAIN CEMENT CONCRETE INFECTED WITH *Aspergillus niger*

Table 4: Weight Loss Percentage of plain cement concrete pieces of control over 1 month.

Test Tube Setup	Weight (g)		Weight Loss (g)	Weight Loss Percentage (%)	Average Weight Loss Percentage (%)
	Initial	Final			
Control	7.686	7.780	0.094	1.223	1.273±0.159
	7.158	7.240	0.082	1.145	
	6.614	6.710	0.096	1.451	
Infected With *Aspergillus niger*	3.122	3.050	0.072	2.306	2.336±0.0635
	5.711	5.580	0.131	2.293	
	4.275	4.172	0.103	2.409	

CONCRETE MATERIAL – PLAIN CEMENT CONCRETE INFECTED WITH *Aspergillus tamarii*

Table 5: Weight Loss Percentage of plain cement concrete pieces of biodeterioration over 1 month.

Test Tube Setup	Weight (g)		Weight Loss (g)	Weight Loss Percentage (%)	Average Weight Loss Percentage (%)
	Initial	Final			
Control	5.571	5.680	0.109	1.956	2.002±0.185
	7.387	7.550	0.163	2.206	
	5.911	6.020	0.109	1.844	
Infected With *Aspergillus tamarii*	4.758	4.610	0.148	3.1105	3.099±0.042
	4.083	3.955	0.128	3.1349	
	6.617	6.415	0.202	3.0527	

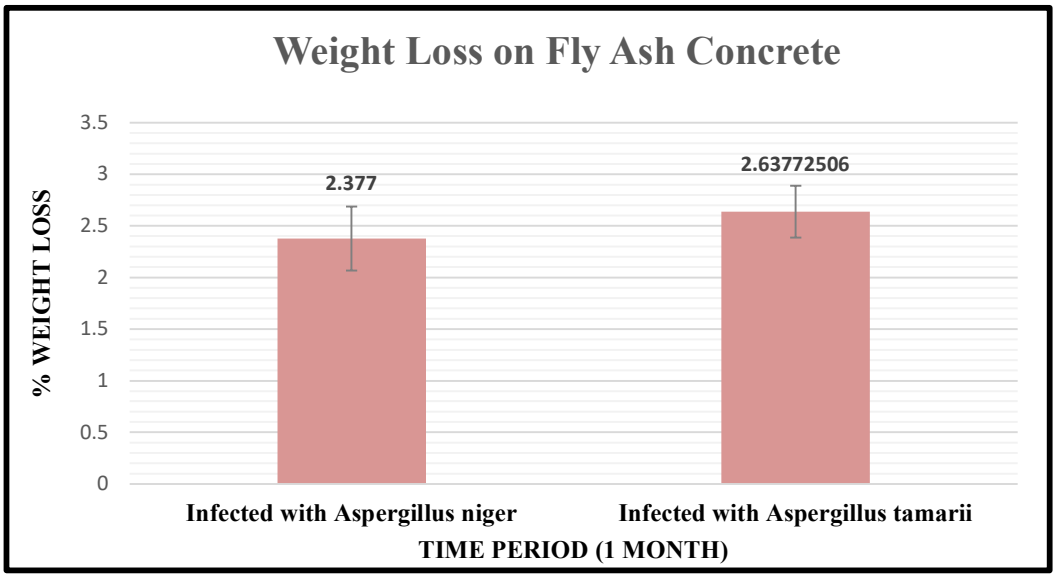

Figure 48: Comparison of Weight Loss Percentage (%) of fly ash concrete pieces between *Aspergillus niger* and *Aspergillus tamarii*

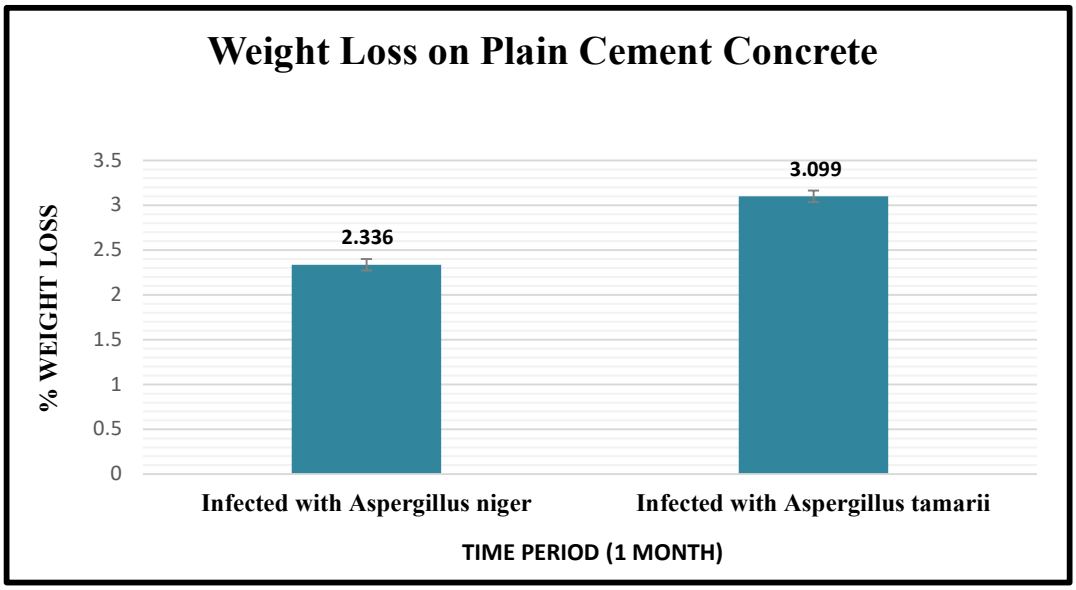

Figure 49: Comparison of Weight Loss Percentage (%) of plain cement concrete pieces between *Aspergillus niger* and *Aspergillus tamarii*

From the above graph, we can see that % weight loss in 1 month by *Aspergillus tamarii* is more than *Aspergillus niger*, so it can be concluded that *Aspergillus tamarii* is more dominant than *Aspergillus niger.*

5.1.1.3 pH measurement (after 1 month study):

FLY ASH CONCRETE PIECES BIODETERIORATION

Table 6: Recorded pH of the biodeteriorated fly ash concrete pieces dipped media.

Name	Initial pH	Final pH (after 1 month)
Control (without infection)	**7.3±0.2**	**7.78**
***Aspergillus niger* infected concrete pieces**	**7.3±0.2**	**8.02**
***Aspergillus tamarii* infected concrete pieces**	**7.3±0.2**	**8.18**

PLAIN CEMENT CONCRETE PIECES BIODETERIORATION

Table 7: Recorded pH of the biodeteriorated plain cement concrete pieces dipped media.

Name	Initial pH	Final pH (after 1 month)
Control (without infection)	**7.3±0.2**	**7.81**
***Aspergillus niger* infected concrete pieces**	**7.3±0.2**	**7.93**
***Aspergillus tamarii* infected concrete pieces**	**7.3±0.2**	**8.26**

The initial pH of the media was 7.3±0.2 but with the proceeding of the study, the pH of the media of both the biodeterioration were noted to have increased making the media more alkaline in nature. An increment in the overall pH for both the cases were thus observed. Luo et al., (2007) studies agreed with this result which shows that when *Trichoderma reesei* interacts with concrete its dissolves $Ca(OH)_2$ (calcium hydroxide) into the growth medium and thus the pH of the media which was 6 initially increased to 13 considerably.

5.2 Tests and Analysis done on the Concrete cubes:

5.1.2 Humidity measurement:

Table 8: Relative Humidity of the atmosphere and inside the set-up boxes for 6 months.

Time Period	ATMOSPHERIC		HUMIDITY (%RH)	
	Temperature (°C)	Humidity (%RH)	PLAIN CEMENT CONCRETE	
			Control	Biodeterioration
Initial	27.3 °C	78.6	71.3	78.6
2nd Month	25.9°C	65.9	71.6	78.9
4th Month	35.4°C	58.3	70.9	77.6
6th Month	33°C	68.0	70.5	79.8

Time Period	ATMOSPHERIC		HUMIDITY (%RH)		
	Temperature (°C)	Humidity (%RH)	FLY ASH CONCRETE		
			Control	Biodeterioration	Prevention
Initial	27.3 °C	78.6	77.5	76.9	79.6
2nd Month	25.9°C	65.9	72.8	75.4	84.2
4th Month	35.4°C	58.3	70.5	73.8	85.2
6th Month	33°C	68.0	69.8	74.6	84.6

The relative humidity was recorded to be the least in the control set-up. Humidity was recorded to be the highest in both the biodeterioration and prevention set-up respectively as a considerable volume of media was added initially to these sets for the optimum growth of the inoculated *Aspergillus tamarii*.

5.2.2 pH measurement :

Table 9:Measured pH value of media inside the set-up boxes for 6 months.

Time Period	pH of the media
	PLAIN CEMENT CONCRETE
	Biodeterioration
Initially	7.3±0.2
After 2 months	7.9
After 4 months	9.4
After 6 months	10.3

Time Period	pH of the media	
	FLY ASH CONCRETE	
	Biodeterioration	**Prevention**
Initially	7.3±0.2	7.3±0.2
After 2 months	7.6	8.1
After 4 months	8.8	9.6
After 6 months	11.4	12

The initial pH of the media was 7.3±0.2 but with the proceeding of the study, the pH of the media of both the biodeterioration and the prevention were noted to have increased making the media more alkaline in nature. An increment in the overall pH for both the cases were thus observed. Luo et al., (2007) studies agreed with this result which shows that when *Trichoderma reesei* interacts with concrete its dissolves $Ca(OH)_2$ (calcium hydroxide) into the growth medium and thus the pH of the media which was 6 initially increased to 13 considerably.

5.2.3 Colour change observation:

The colour change detected in both the concrete cubes (Plain cement concrete and Fly ash concrete) over time were inferred with the help of the Geological Rock Colour Chart (Munsell, 2009). It was observed that the growth of the fungal species, on the concrete cubes of the biodeterioration and the prevention sets, imparted a significant greenish hue (Light greenish gray) to the cubes which eventually turned to a shade of yellowish gray with longer exposure time.

However, the concrete cubes of the control sets retained their original colour (Pinkish gray) throughout the experiment.

PLAIN CEMENT CONCRETE

Control:

2nd Month
Pinkish gray
(5YR 8/1)

4th Month
Pinkish gray
(5YR 8/1)

6th Month
Pinkish gray
(5YR 8/1)

Biodeterioration by *Aspergillus tamarii* :

2nd Month
Light greenish gray
(5GY 8/1)

4th Month
Yellowish gray
(5Y 8/1)

6th Month
Yellowish gray
(5Y 8/1)

Figure 50: Observed colour change of the plain cement concrete cube surfaces along with their respective colour codes (as per Geological Rock Colour chart – Munsell, 2009).

FLY ASH CONCRETE

Control:

2nd Month
Pinkish gray
(5YR 8/1)

4th Month
Pinkish gray
(5YR 8/1)

6th Month
Pinkish gray
(5YR 8/1)

Biodeterioration by *Aspergillus tamarii* :

2nd Month
Light greenish gray
(5GY 8/1)

4th Month
Yellowish gray
(5Y 8/1)

6th Month
Yellowish gray
(5Y 8/1)

Prevention:

2nd Month
Light greenish gray
(5GY 8/1)

2nd Month
Light greenish gray
(5GY 8/1)

6th Month
Light greenish gray
(5GY 8/1)

Figure 51: Observed colour change of the fly ash concrete cube surfaces along with their respective colour codes (as per Geological Rock Colour chart – Munsell, 2009).

5.2.4 Weight loss measurement:

CONTROL SETUP – PLAIN CEMENT CONCRETE

Table 10: Weight loss Percentage (%) for Control set-up.

Time Period	Weight (kg)		Weight Loss (kg)	Weight Loss Percentage (%)	Average Weight Loss Percentage (%)
	Initial	Final			
After 2 months	2.550 2.375 2.445	2.547 2.374 2.443	0.003 0.001 0.002	0.117 0.042 0.081	0.080±0.037
After 4 months	2.410 2.390 2.400	2.399 2.380 2.390	0.011 0.010 0.010	0.456 0.418 0.417	0.430±0.022
After 6 months	2.360 2.355 2.400	2.340 2.335 2.390	0.020 0.020 0.010	0.847 0.849 0.417	0.704±0.249

BIODETERIORATION SETUP – PLAIN CEMENT CONCRETE

Table 11: Weight loss Percentage (%) for Biodeterioration set-up.

Time Period	Weight (kg)		Weight Loss (kg)	Weight Loss Percentage (%)	Average Weight Loss Percentage (%)
	Initial	Final			
After 2 months	2.445 2.445 2.44	2.439 2.440 2.438	0.006 0.005 0.002	0.24539 0.20449 0.08196	0.177±0.085
After 4 months	2.44 2.345 2.375	2.420 2.330 2.360	0.020 0.015 0.015	0.81967 0.63966 0.63758	0.696±0.106
After 6 months	2.43 2.45 2.365	2.395 2.415 2.336	0.035 0.035 0.029	1.44039 1.42857 1.22622	1.365±0.120

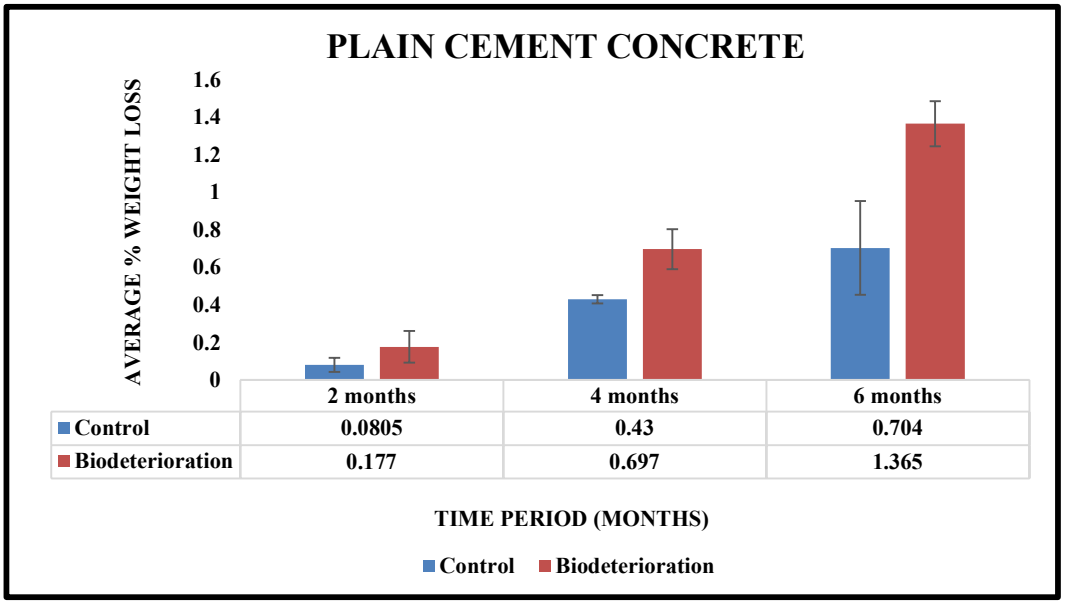

Figure 52: Comparison of percentage weight loss (%) with time (months) of concrete cubes.

From the data tables and the column graph, it was inferred that over the period of 6 months the concrete cubes of each experimental set have undergone weight loss with variation in each of the set-ups. The weight loss in biodeteriorated concrete cubes were observed to be the highest, followed by control cubes.

CONTROL SETUP – FLY ASH CONCRETE

Table 12: Weight loss Percentage (%) for Control set-up.

Time Period	Weight (kg)		Weight Loss (kg)	Weight Loss Percentage (%)	Average Weight Loss Percentage (%)
	Initial	Final			
After 2 months	2.435 2.375 2.435	2.428 2.371 2.432	0.007 0.004 0.003	0.28747 0.16842 0.12320	0.193±0.084
After 4 months	2.455 2.390 2.485	2.435 2.380 2.464	0.002 0.010 0.021	0.81466 0.41841 0.84507	0.693±0.238
After 6 months	2.405 2.380 2.425	2.390 2.365 2.415	0.015 0.015 0.010	0.62370 0.63025 0.41237	0.555±0.123

BIODETERIORATION SETUP – FLY ASH CONCRETE

Table 13: Weight loss Percentage (%) for Biodeterioration set-up.

Time Period	Weight (kg)		Weight Loss (kg)	Weight Loss Percentage (%)	Average Weight Loss Percentage (%)
	Initial	Final			
After 2 months	2.455 2.490 2.455	2.442 2.480 2.443	0.013 0.010 0.012	0.5350 0.4010 0.4880	0.473±0.065
After 4 months	2.400 2.355 2.390	2.370 2.320 2.360	0.030 0.035 0.030	1.2500 1.4862 1.2552	1.330±0.134
After 6 months	2.440 2.420 2.485	2.410 2.390 2.455	0.030 0.030 0.030	1.2350 1.2460 1.2072	1.234±0.016

PREVENTION SETUP – FLY ASH CONCRETE

Table 14: Weight loss Percentage (%) for Prevention set-up.

Time Period	Weight (kg)		Weight Loss (kg)	Weight Loss Percentage (%)	Average Weight Loss Percentage (%)
	Initial	Final			
After 2 months	2.395 2.440 2.395	2.387 2.435 2.386	0.008 0.005 0.009	0.3340 0.2049 0.3757	0.304±0.089
After 4 months	2.465 2.435 2.320	2.440 2.410 2.300	0.025 0.025 0.020	1.0141 1.0266 0.8620	0.967±0.091
After 6 months	2.390 2.385 2.425	2.370 2.370 2.400	0.020 0.015 0.025	0.8368 0.6289 1.0309	0.832±0.201

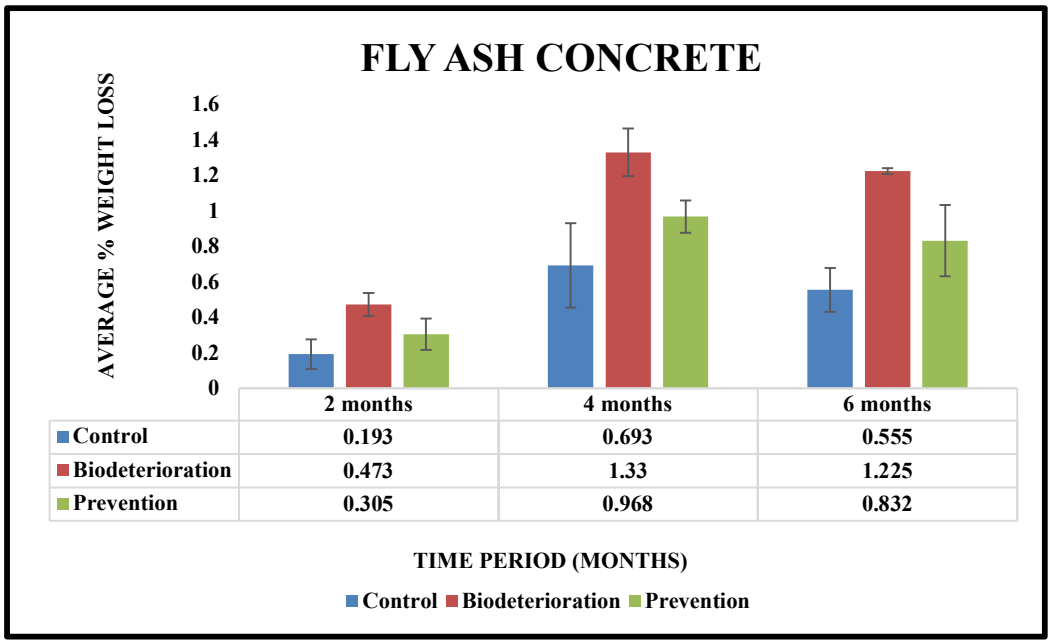

Figure 53: Comparison of percentage weight loss (%) with time (months) of concrete cubes.

From the data tables and the column graph, it was inferred that over the period of 6 months the concrete cubes of each experimental set have undergone weight loss with variation in each of the set-ups. The weight loss in biodeteriorated cubes were observed to be the highest followed by nanocoated cubes and control cubes.

The weight loss percentage result agreed with some similar studies conducted by Gu et al., (1998), and Harbulakova et al., (2013) which concluded that biodeterioration of concrete resulted in their weight loss. The study done by Harbulakova et al., (2013) also concluded that the concrete when kept in distilled water showed almost negligible changes in weight over time.

Moreover the loss of weight in concrete cubes of control can be explained with the study conducted by Gesoglu et al.,(2015), stating that drying shrinkage, which is the loss of absorbed water in concrete with time, affects its weight adversely. It was also deduced that this volumetric change in concrete depended on the drying duration, water to cement ratio, cement composition, aggregate properties, admixtures, curing temperature, degree of hydration and relative humidity.

5.2.5 Stereo Microscope :

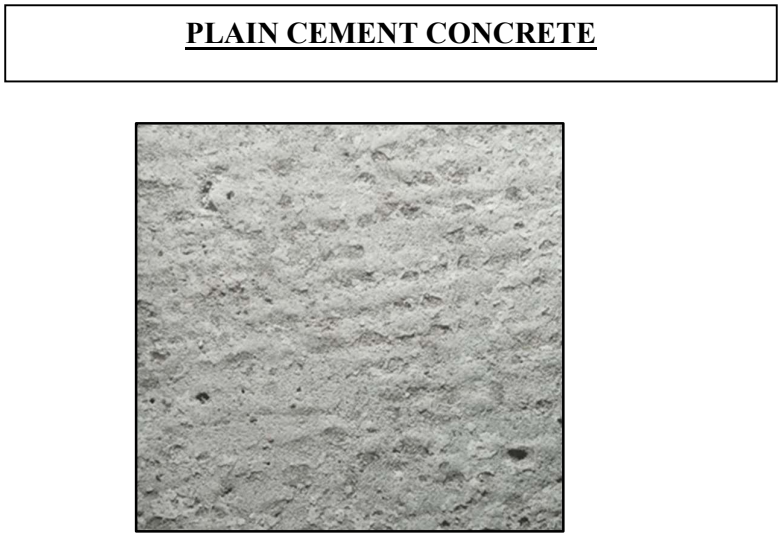

Figure 54: Stereo microscopic image of concrete cube surface from the control set-up.

Figure 55: Stereo microscopic images of concrete cube surfaces infected by fungus from the biodeterioration set-up.

FLY ASH CONCRETE

Figure 56: Stereo microscopic image of concrete cube surface from the control set-up.

z

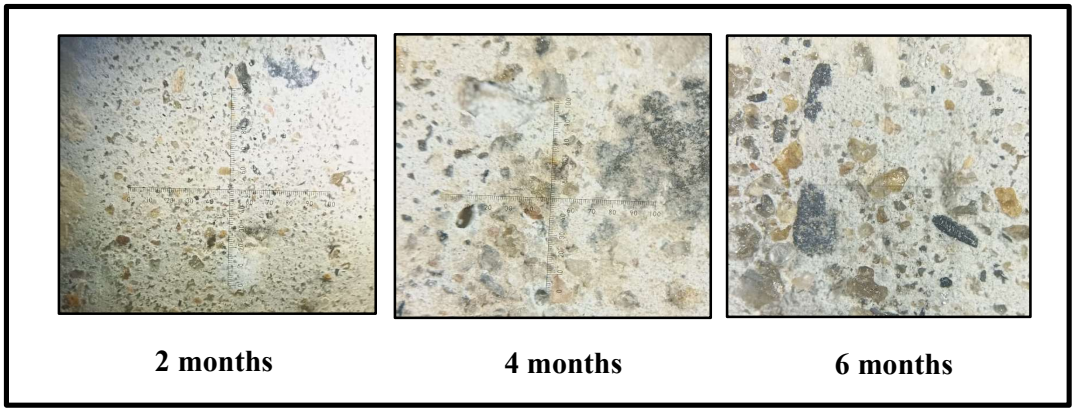

Figure 57: Stereo microscopic images of concrete cube surfaces infected by fungus from the biodeterioration set-up.

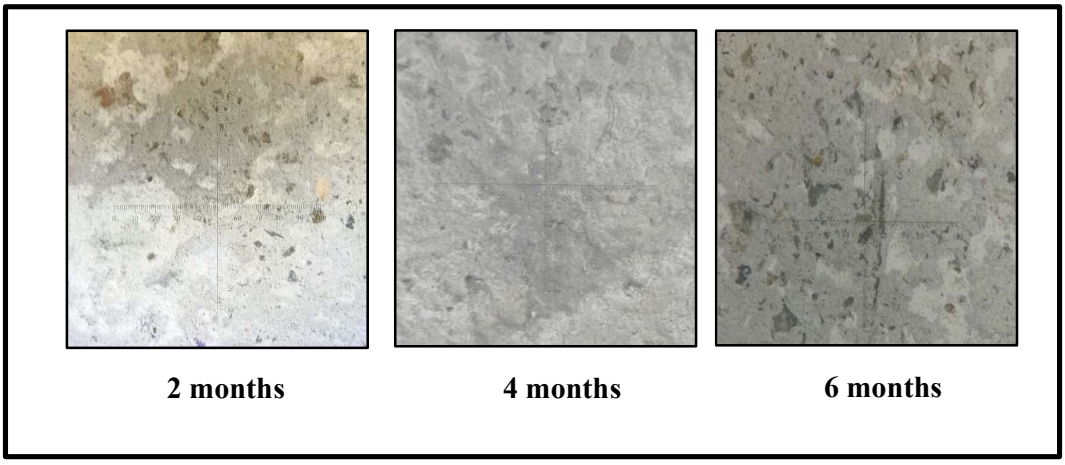

Figure 58: Stereo microscopic images of concrete cube surfaces infected by fungus from the prevention set-up.

As compared to control, the concrete surface of the biodeterioration as well as of prevention were seen to have got exposed and rough. The growth of micro-organisms on concrete exposes the concrete surface thus increasing the porosity and reducing the protective layer that covers the concrete surface, making it vulnerable to cracking and other mechanical damages (Sanchez et al.,2008).

The intensity of roughness was observed more in biodeteriorated concrete cubes rather than in the nanocoated ones under the stereo microscope. The surface of the cubes of biodeterioration developed cavities as can be seen in the images (Figure 30). Concrete is more susceptible to microbiological attack with a high rate of fungal growth mainly because of its initial porosity and chemical composition. In the case of nanocoated concrete cubes, the coating provided a surface protective layer (Aldosari et al., 2018) which inhibited the growth of the fungus to a considerable limit thus revealing much less of the concrete cube surface.

5.2.6 Compressive strength test:

PLAIN CEMENT CONCRETE - M25 GRADE

Initial: (After 28 days curing followed by drying for 3 days)

Table 15: Initial Compressive strength of plain cement concrete cubes.

Peak Load (kN)	Initial Compressive Strength (N/mm^2)	Average Compressive Strength (N/mm^2)
156.2	25.64	28.94
147.4	30.5	
146.7	30.7	

Control

Table 16: Peak load and Compressive Strength of concrete cubes from Control set-up.

Time Period	Peak Load (kN)	Compressive Strength(N/mm^2)	Average Compressive Strength (N/mm^2)
After 2months	157.6 149.2 152.8	31.65 30.98 31.20	31.27±0.341
After 4months	170.4 155.3 166.6	33.63 32.56 34.16	34.45±0.815
After 6months	148.8 159.5 167.4	38.23 37.26 39.49	40.32±1.118

Biodeterioration

Table 17: Peak load and Compressive Strength of concrete cubes from Biodeterioration set-up.

Time Period	Peak Load(kN)	Compressive Strength(N/mm^2)	Average Compressive Strength (N/mm^2)
After 2months	160.6 149.5 134.3	29.65 30.78 31.23	30.55±0.814
After 4months	142.6 184.4 182.9	30.6 32.59 33.98	32.05±1.7
After 6months	152.7 179.0 185.5	33.45 34.2 33.96	33.87±0.383

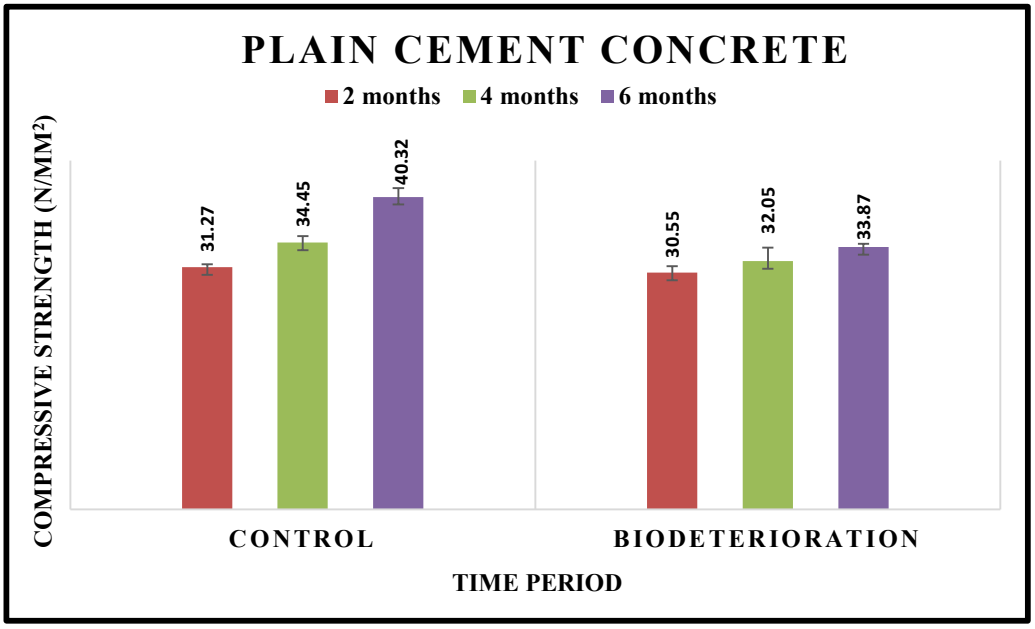

Figure 59: Comparison of compressive strength of concrete cubes with time from the respective experimental set-ups.

FLY ASH CONCRETE - M25 GRADE

Initial : (After 28 days curing followed by drying for 3 days)

Table 18: Initial Compressive strength of fly ash concrete cubes.

Peak Load (kN)	Initial Compressive Strength (N/mm^2)	Average Compressive Strength (N/mm^2)
156.2	28.95	30.55
147.4	31.08	
146.7	31.67	

Control

Table 19: Peak load and Compressive Strength of concrete cubes from Control set-up.

Time Period	Peak Load(kN)	Compressive Strength(N/mm^2)	Average Compressive Strength (N/mm^2)
After 2months	159.6 149.5 137.3	30.45 31.69 31.98	31.37±0.813
After 4months	156.6 184.4 183.9	33.59 34.17 35.26	36.34±0.847
After 6months	152.7 181.0 185.5	39.29 37.49 38.26	42.35±0.903

Biodeterioration

Table 20 : Peak load and Compressive Strength of concrete cubes from Biodeterioration set-up.

Time Period	Peak Load(kN)	Compressive Strength(N/mm^2)	Average Compressive Strength (N/mm^2)
After 2months	153.6 149.5 151.3	30.45 30.69 30.98	30.70±0.265
After 4months	176.6 184.4 173.9	32.59 31.17 34.26	32.68±1.546
After 6months	172.7 171.0 185.5	33.29 35.49 36.12	34.97±1.485

Prevention

Table 21: Peak load and Compressive Strength of concrete cubes from Prevention set-up.

Time Period	Peak Load(kN)	Compressive Strength(N/mm^2)	Average Compressive Strength (N/mm^2)
After 2months	143.6 159.5 153.3	31.56 30.87 31.25	31.23±0.345
After 4months	174.6 185.4 178.9	33.25 34.59 34.14	34.99±0.681
After 6months	182.7 168.0 185.5	36.97 35.87 35.89	39.24±0.630

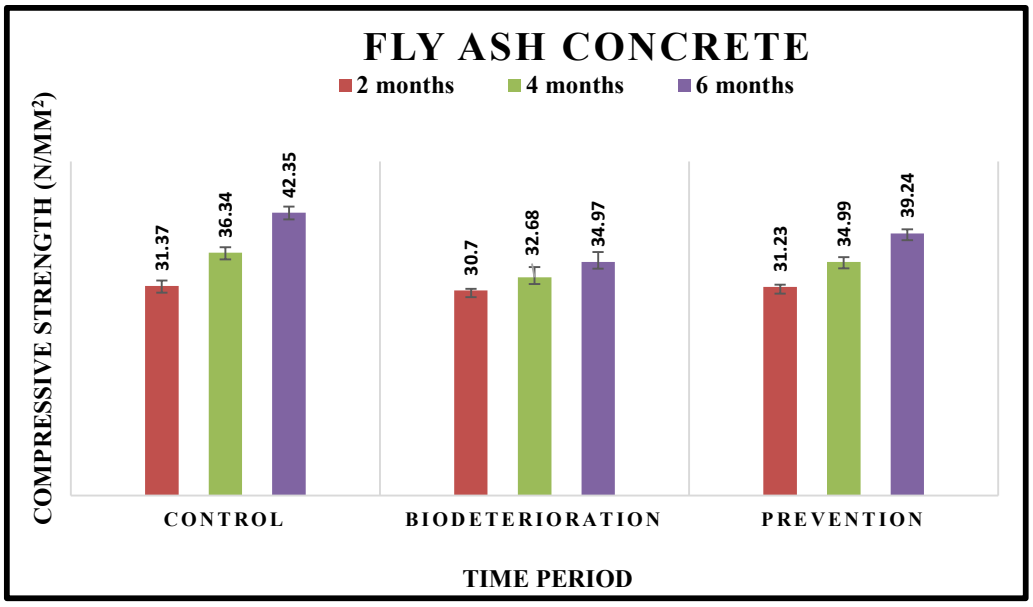

Figure 60: Comparison of compressive strength of concrete cubes with time from the respective experimental set-ups.

An increase in the compressive strength from the initial compressive strength was observed in all the concrete specimens. For the control, where the fungal activity was absent, the compressive strength increase was observed to be the highest followed by nanocoated concrete cubes. The compressive strength increase of biodeteriorated cubes were the least of all the specimens.

This gradual increment in compressive strength in biodeterioration, prevention and control set-up could be justified by the reason that all the cubes of these set-ups were kept in an environment where the facilitation of continuous hydration was possible. Hydration is the process consisting of chemical reaction series that occurs between the cement and water, where the water molecules and the major components of cement forms chemical bonds to harden the concrete. In the study, the cubes kept in aqueous media in control, biodeterioration and prevention sets stimulated the process of hydration thus resulting in the rise of compressive strength overthe time period of 6 months. In a study conducted by Harbulakova et al.,(2013) , a similarkind of result was observed, where the concrete cubes were immersed in wastewater and their compressive strength increased with time.

Moreover they found that the biocorrosion activity on their high grade concrete cubes was more prominent after a longer exposure (18 months) of the cubes to the wastewater which resulted in an enormous drop in the compressive strength.

Also from the data, the compressive strength increase of nanocoated cubes was noted to be higher than that of the biodeteriorated cubes. Application of organic polymer layer on concrete may not prevent the growth of fungus completely as it can not only get degraded easily but also can provide a susceptible environment for the fungus to grow (Aldorasi el al., 2018). The incorporation of inorganic nanoparticle in a polymer improves the barrier property which slows down the degradation of the polymer (Pan et al., 2017) thus slowing down the fungal growth. This infers that the nanocoating provided an inhibition layer for the fungus to affect the cube much less adversely as compared to the biodeteriorated one which in turn affects its compressive strength.

5.2.7 Fourier Transform Infrared Spectroscopy (FTIR):

PLAIN CEMENT CONCRETE

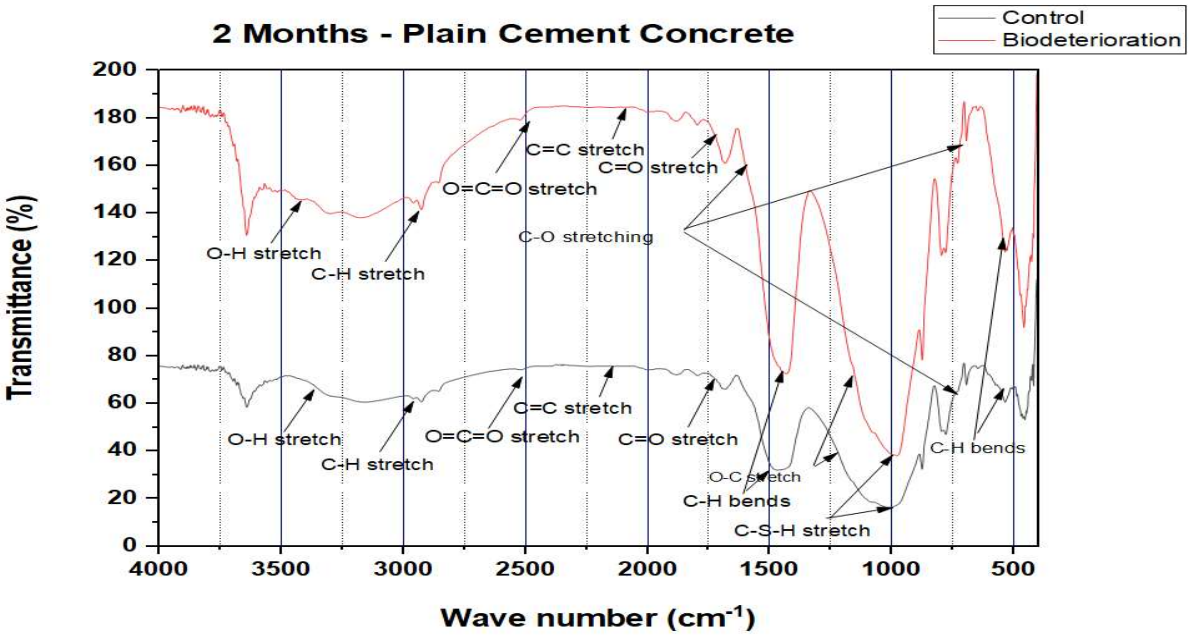

Figure 61 IR transmittance spectrum of plain cement concrete (2 months).

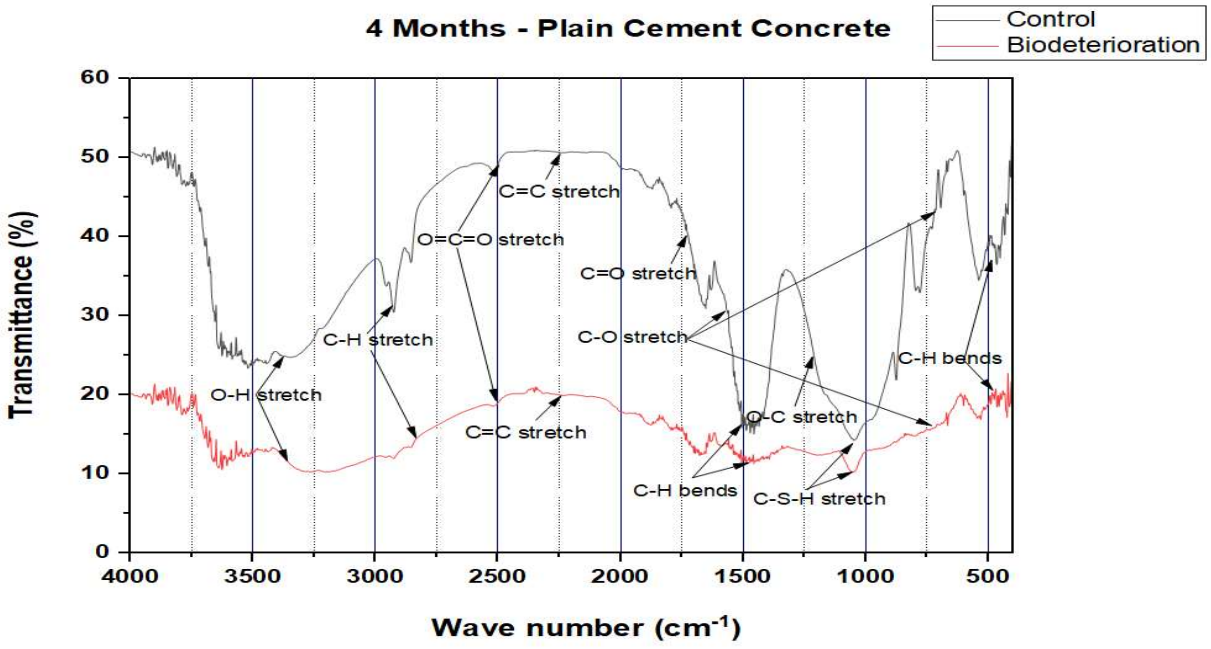

Figure 62: IR transmittance spectrum of plain cement concrete (4 months).

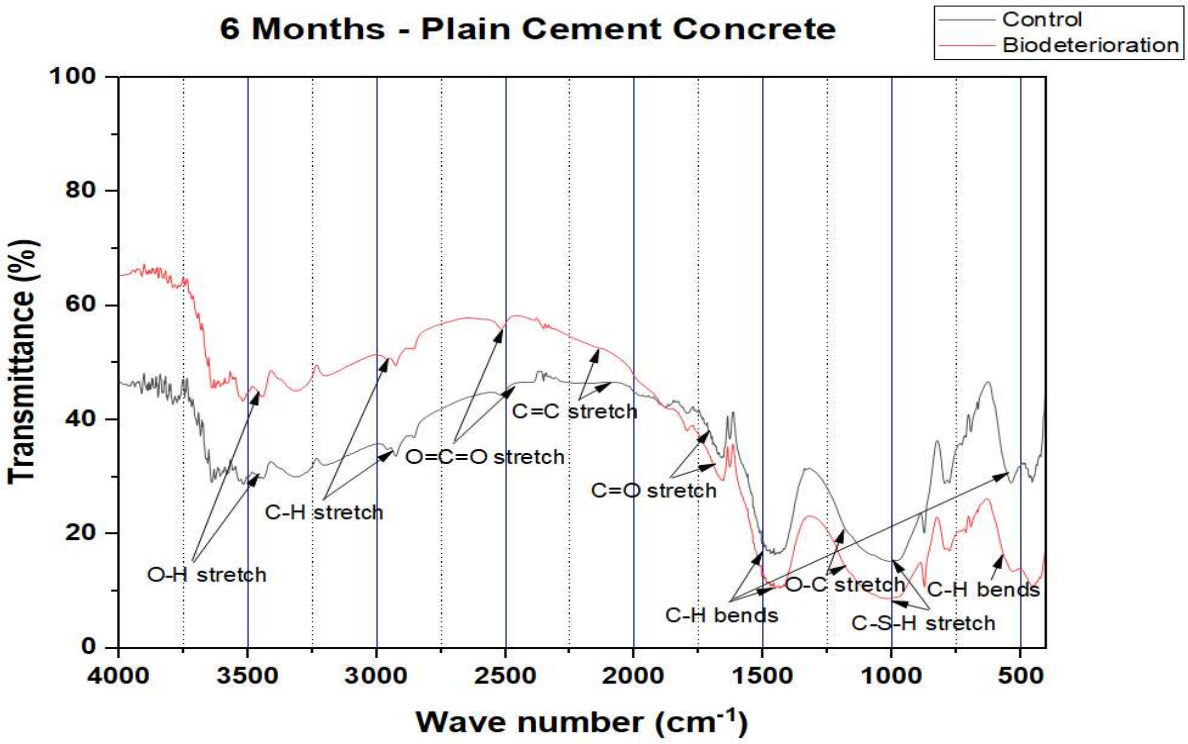

Figure 63: IR transmittance spectrum of plain cement concrete (6 months).

From the graphs, a mid IR regional (500-4000 cm^{-1}) spectrum can be visualized. This is ideal for the interpretation of the fundamental structures of specimens and the localization of prominent delineated absorption bands of organic functional groups. According to the IR Correlational chart (Derrick et al.,1955), The spectrum is mainly divided into two regions based on the wavenumber (cm^{-1}). The bands detected in the range of 4000 cm^{-1} to 1300 cm^{-1} falls in the group frequency region whereas the bands detected in the range of 1300 cm^{-1} to 500 cm^{-1} falls in the fingerprint region. Hydrogen stretching vibrations consisting of only two atoms shows their principal absorptions bands from 4000 cm^{-1} to 2500 cm^{-1}. The intermediate frequency range of 2500 cm^{-1} to 1500 cm^{-1} shows the unsaturated region which primarily consists of triple bond frequencies (2500 cm^{-1} to 2000 cm^{-1}) and double bond frequencies (2000 cm^{-1} to 1540 cm^{-1}). Many functional group bands can also be detected in the 1350 cm^{-1} to 650 cm^{-1} frequency.

The FTIR spectroscopy for control concrete sample indicated the presence of portlandite [$Ca(OH)_2$;] at range of 3640 cm^{-1} to 3250 cm^{-1} (very weak O-H stretching vibrations) which are present in both the samples (control and biodeterioration) but for biodeterioration sample the curved got sharper with time, it means that Portlandite is mainly transformed during carbonation and leaching process. The carbonation of Portland cement is a natural process during the ageing of concrete. During the carbonation process $CaCO_3$, was formed. Carbonate such as calcite ($CaCO_{.3}$) from C-O stretching showed a strong symmetric absorption band (1400 and 874 cm) which became flatten in fungi infected concrete samples with time. This band can be misleading because of absorbed water on the sample. Hydrogen bonding can change the band position and shape. Very weak stretching band (C=C) is present at range of (2000-1500) cm^{-1} and with time the curved peaks are getting closer for both the samples. Another asymmetric stretching band C-H was strong at initial stage which became medium and very weak in fungal infected concrete sample. A weak asymmetric stretching band from C-S-H of crystalline silica mineral quartz (Si-O) was observed at 980 cm to 1000 cm^3, which became very weak after fungal deterioration study with time. Some of other bands like C-H , C=O and O-C were also present in the control sample which became medium in fungal infected concrete sample because these bands were weakened and subsequently broken by the action of fungi with time. It depends on pH, texture, mineral constituents and relative percentage of mineral constituents of concrete. This had direct relationship with the difference in weight loss and compressive strength loss in fungal infected samples. As the bands became weak or got disappeared, the hydration products were changed which also resulted in weakening of the matrix and thereby cracks were formed. Water and other salts percolation through these cracks initiated corrosion. Therefore, the weight and compressive strength were decreased.

FLY ASH CONCRETE

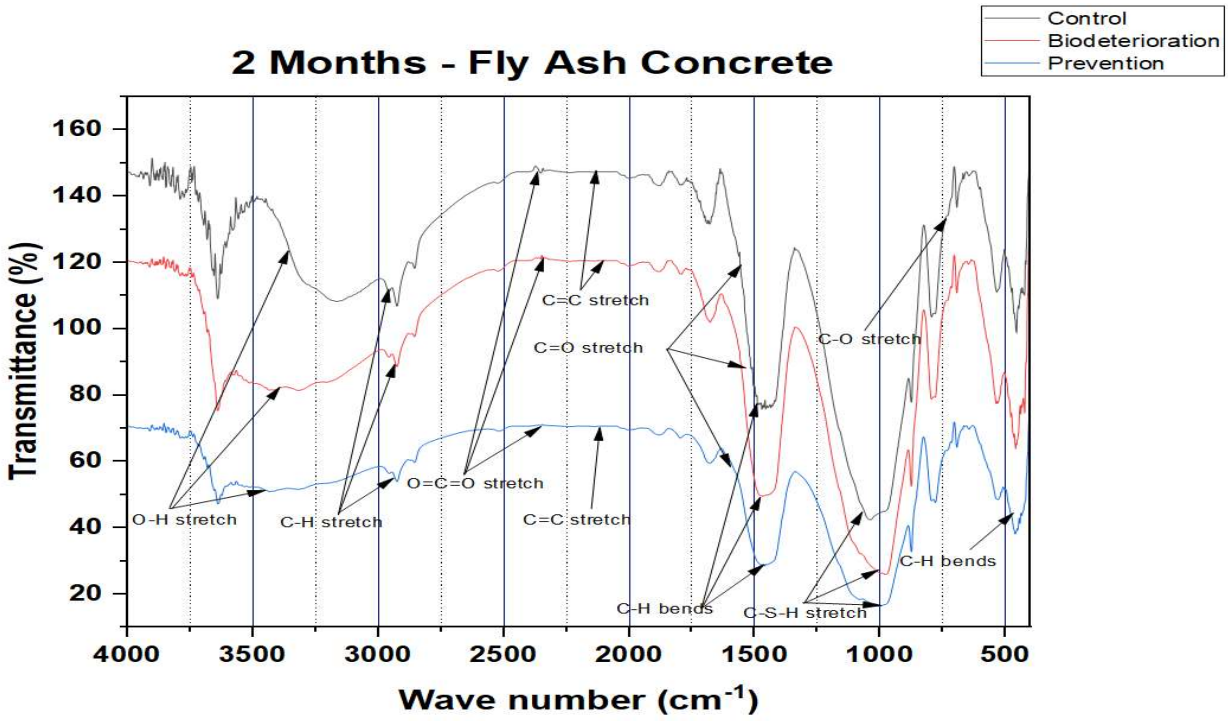

Figure 65: IR transmittance spectrum of fly ash concrete (2 months).

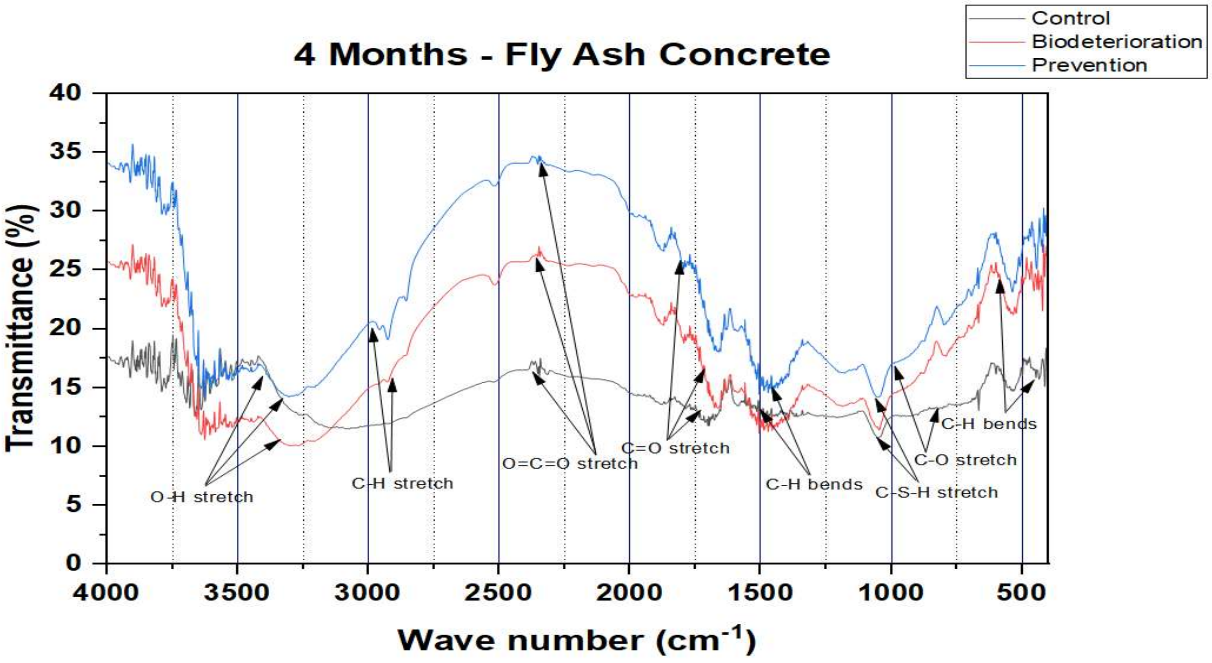

Figure 64: IR transmittance spectrum of fly ash concrete (4 months).

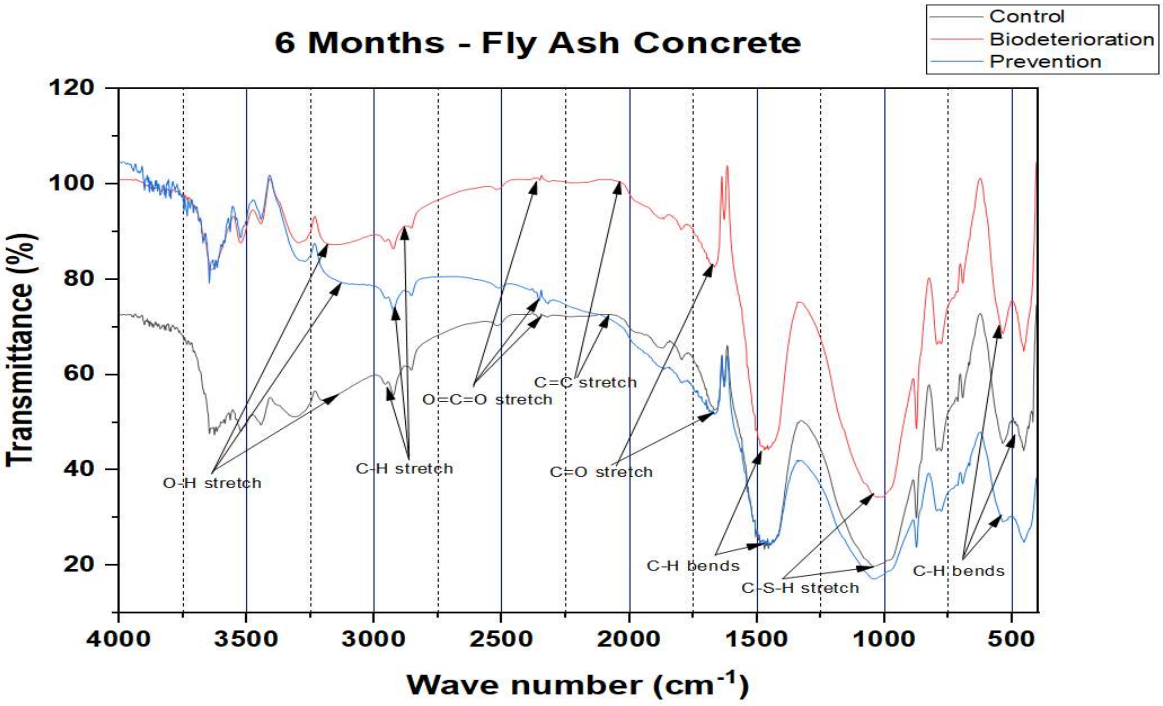

Figure 66: IR transmittance spectrum of fly ash concrete (6 months).

From the graphs, a mid IR regional (500-4000 cm^{-1}) spectrum can be visualized. This is ideal for the interpretation of the fundamental structures of specimens and the localization of prominent delineated absorption bands of organic functional groups. According to the IR Correlational chart (Derrick et al.,1955), The spectrum is mainly divided into two regions based on the wavenumber (cm^{-1}). The bands detected in the range of 4000 cm^{-1} to 1300 cm^{-1} falls in the group frequency region whereas the bands detected in the range of 1300 cm^{-1} to 500 cm^{-1} falls in the fingerprint region. Hydrogen stretching vibrations consisting of only two atoms shows their principal absorptions bands from 4000 cm^{-1} to 2500 cm^{-1}. The intermediate frequency range of 2500 cm^{-1} to 1500 cm^{-1} shows the unsaturated region which primarily consists of triple bond frequencies (2500 cm^{-1} to 2000 cm^{-1}) and double bond frequencies (2000 cm^{-1} to 1540 cm^{-1}). Many functional group bands can also be detected in the 1350 cm^{-1} to 650 cm^{-1} frequency.

Broad envelope type bands centered around 3400 cm^{-1} represents hydroxyl groups. The presence of very broad bands in this region in all the spectral graphs of the tested specimens infers the presence of carboxylic acids. The bands in the biodeterioration were less broad as compared to those of the ones in prevention spectral graphs.

The region of 3200 cm^{-1} to 2800 cm^{-1} is known as the C-H stretching region. The prominent stretching (3000 cm^{-1} to 2890 $cm^{-}1$) seen in all the spectral graphs of the specimens infers the presence of saturated carbon groups such as methyl and methylene (both symmetric and asymmetric) groups. The sharp C-H stretches in control IR spectrum near 2925 cm^{-1} and 2850 cm^{-1} indicates the presence of both symmetric and asymmetric methylene groups. Similar sharp peaks are can be noticed in the IR spectrums of the biodeteriorated and nanocoated cubes from the biodeterioration and prevention set-ups respectively, which can be seen to get sharper after 4 months and 6 months.

In the window region extending from 2800 cm^{-1} to 1800 cm^{-1}, atmospheric carbon dioxide or O=C=O stretch at 2340 cm^{-1} can be seen in all the specimens. Here also the sharp doublets can be seen to gradually sharper after 4 months and 6 months in biodeterioration and prevention.

The carbon double bond region (1800 cm^{-1} to 1500 cm^{-1}) showing the presence of C=O in all the specimens as well as in control.

The nature of the IR spectrums of control and the specimens showed significant chemical changes that occurred after the fixed intervals of time.

5.2.8 Energy Dispersive X-Ray Fluorescence Spectroscopy (EDXRF) :

PLAIN CEMENT CONCRETE

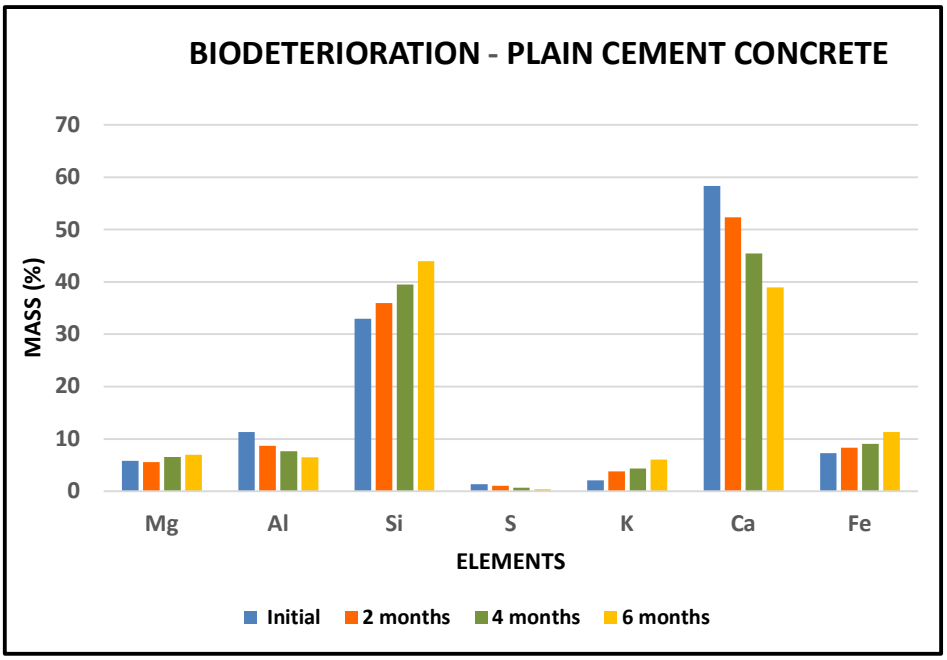

Figure 67: Mass percentage of different elemental contents of biodeteriorated plain cement concrete cubes.

FLY ASH CONCRETE

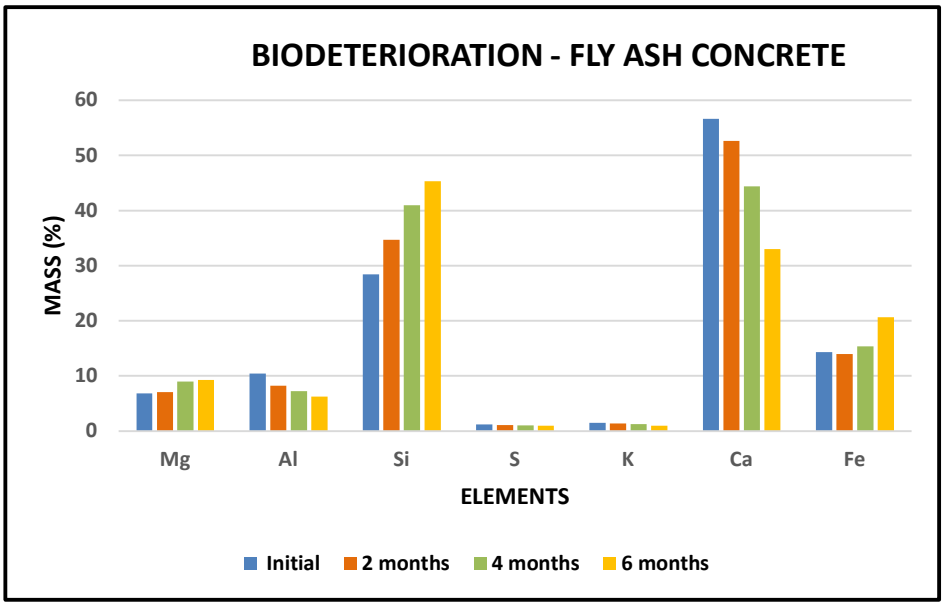

Figure 68: Mass percentage of different elemental contents of biodeteriorated fly ash concrete cubes.

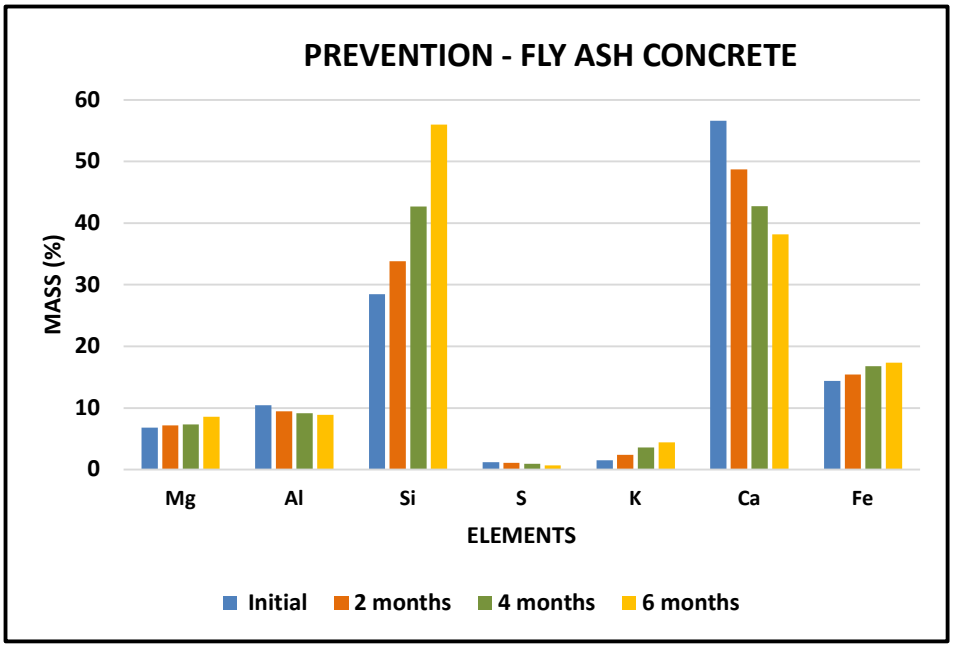

Figure 69: Mass percentage of different elemental contents of prevention set of fly ash concrete cubes.

According to the EDXRF results the major elements whose composition variability was prominently detected were silicon, calcium, magnesium, iron, sulphur and potassium. The composition of titanium in all the specimens were detected but its compositional change was minimal as compared to the rest. Apart from these, trace amounts of copper, manganese, zinc, chromium and nickel were noted initially but these eventually disappeared with time. The main sources of the detected major elements in concrete are: silicon from Portland cement and sand (SiO_2), calcium, magnesium and iron from Portland cement, and sulphur from gypsum used in Portland cement.

The decrease in mass fraction (%) of calcium was due to the fungal activity of *Aspergillus tamarii* on both the sets of biodeteriorated and nanocoated cubes. In a study conducted by Adeyemi et al., (2005), fungal growth of three different species which included *Aspergillus niger* on mineral rocks of apatite, galena and obsidian showed that organic acids (oxalic and malic acid) produced by the hyphae of these fungi helped in the dissolution of calcium along with the precipitation of crystals of calcium oxalates. However, the rate of decrease of calcium in nanocoated concrete cubes as compared to that of biodeteriorated ones shows that the silicon dioxide nanocoating to some extent provided a barrier for the complete dissolution action of these organic acids upon concrete. Though biological processes and alike stimulates the weathering of silica and silicates from rocks (Brehm et al., 2005), silicon compounds such as aluminosilicates, may inhibit the metabolism of microbes (Marshman & Marshall, 1981). Fomina et al., (2007c) obtained that species of *Alternaria, Cladosporium and Aspergillus* colonizing the concrete utilized for radioactive waste barrier in Chernobyl facilitated the leaching of calcium, silicon, aluminum, and iron and in their micro environment reprecipitated siliconand calcium.

Grayston and Wainwright (1987) obtained that *Aspergillus niger* and *Trichoderma harzanium* in mixed culture with *Mucor flavus* and various other soil fungi, had the ability to oxidize elemental sulphur into thiosulphate and sulphate in vitro. This may account for the slight fall in mass fraction of sulphur.

Another study conducted by Fomina et al.,(2004) suggested that the fungus *Beauveria caledonica* through a ligand-promoted mechanism of over excreted organic acids, solubilized copper, cadmium, zinc and lead into their corresponding oxides. This explains the gradual amount decrement of zinc and copper in the study.

CHAPTER VI

CONCLUSION

It was observed that the concrete pieces of the biodeterioration set-up over the time lost its original colour (as could be seen in control) and after infection with fungus it became more paler and rustier in case of *Aspergillus tamarii* than *Aspergillus niger*.

The assessment of growth of the fungal species, *Aspergillus tamarii* and its effects on concrete followed by its effective prevention using silicon oxide nanoparticles was thoroughly and successfully investigated for a period of 6 months.

The results of the investigation concluded that:

pH: - media of biodeterioration showed more alkalinity than the prevention set-up due to more leaching and dissolution of $Ca(OH)_2$ due to fungal activity in both the building material. Hence it was inferred that the fungal deterioration was higher in the biodeteriorated concrete cubes than the nanocoated concrete cubes.

Colour Change Observation: - It was observed that the concrete cubes of the biodeterioration set-up over the time lost its original colour after infection with fungus it became more paler and rustier in case of biodeterioration than in prevention setup for both the building materials.

Weight Loss Percentage: -The weight loss in case of plain cement concrete shows higher weight loss percentage for biodeterioration setup than for control setup and in case of fly ash concrete shows higher weight loss percentage for biodeterioration setup followed by prevention setup then for control setup.

Stereo microscope: - The images obtained from the stereo microscope showed clear exposure and roughening of the surface in biodeterioration cubes more than those of the nanocoated cubes.

Compressive strength test: - The compressive strength values got increased for both the building material. In case of plain cement concrete, the % of increment for control setup was found to be highest followed by biodeterioration setup. And in case of fly ash concrete same type of result were seen, the % of increment for control setup was found to be highest followed by prevention setup and then for control setup.

FTIR:- The analysis showed the redistribution of chemical bonds in the concrete cubes with time. Different types of bends and stretches were identified and marked for the different experimental setups. The nature of the IR spectrums of control and the specimens showed significant chemical changes that occurred after the fixed intervals of time.

Micro EDXRF: -The analysis showed the redistribution of elements in the concrete cubes with time. In EDXRF it was seen that the amount of calcium leaching out in biodeterioration was higher than that of the nanocoated cubes.

Thus from the experimental evidences and results the nanocoating which was applied on the concrete cubes having the binder, nanoparticles and water ratio of 1:0.5:2, was found to be effective against the biodeterioration of the concrete cubes.

CHAPTER VII

FUTURE SCOPE OF STUDY

This investigation of fungal biodeterioration on concrete and its prevention using nanoparticles can be a helpful source of various further studies soon. There is a scope for the following activities that could be carried out regarding this field of topic namely:

I. Biodeterioration study of concrete by other microbial communities can be examined.

II. Other prospects and techniques regarding prevention of fungal biodeterioration of concrete can be studied.

III. If the time period of the investigation can be further extended, then better and more accurate results of fungal attack along with its prevention can be researched.

IV. The binder, nanosilica powder and water ratio along with the number of coatings on concrete can be standardized to increase their effectivity to prevent fungal attack on concrete.

V. We can do the elemental analysis of the sample leached by fungus after deterioration in the media.

VI. The use of an alternate binder instead of polyethylene glycol can be researched to enhance the effectiveness of nano silica.

VII. The effectiveness of other inorganic nanoparticles on prevention concrete biodeterioration due to fungus can be studied.

VIII. The examination of concrete pieces under Scanning Electron Microscope which will show the hyphae and spore developed with time and the colonization of *Aspergillus tamarii* on the concrete surface.

IX. We can cast concrete beam or slab to measure the flexural strength of concrete (tensile strength of unreinforced concrete).

REFERENCES

Adeyemi, A. O., & Gadd, G. M. (2005). Fungal degradation of calcium-, lead-and silicon-bearing minerals. *Biometals*, *18*(3), 269-281.

Aldoasri, M.A., Darwish, S.S., Adam, M.A., Elmarzugi, N.A. and Ahmed, S.M., 2017. Protecting of marble stone facades of historic buildings using multifunctional TiO_2 nanocoatings. Sustainability, 9(11), p.2002.

Aldoasri, Mohammad A., et al. "Protecting of Marble Stone Facades of Historic Buildings Using Multifunctional TiO2 Nanocoatings." *Sustainability* 9.11 (2017): 2002.

Aldosari, M. A., Darwish, S. S., Adam, M. A., Elmarzugi, N. A., & Ahmed, S. M. (2019). Using ZnO nanoparticles in fungal inhibition and self-protection of exposed marble columns in historic sites. *Archaeological and Anthropological Sciences*, 1- 16.

Allsopp, Dennis, Kenneth J. Seal, and Christine C. Gaylarde. *Introduction to biodeterioration*. Cambridge University Press, (2004) : 1-5, 35-43, 203-223.

Andersen, B., Frisvad, J. C., Søndergaard, I., Rasmussen, I. S., & Larsen, L. S. (2011). Associations between fungal species and water-damaged building materials. *Appl. Environ. Microbiol.*, *77*(12), 4180-4188.

Becerra, J., Zaderenko, A. P., Sayagués, M. J., Ortiz, R., & Ortiz, P. (2018). Synergyachieved in silver-TiO 2 nanocomposites for the inhibition of biofouling on limestone. *Building and Environment*, 141, 80-90.

Bertron, A. (2014). Understanding interactions between cementitious materials and microorganisms: a key to sustainable and safe concrete structures in various contexts. *Materials and Structures*, *47*(11), 1787-1806.

Bhattacharyya, S., Akhtar, S., Chaudhuri, A., Mahanty, S., Chaudhuri, P. and Sudarshan, M., 2022. Affirmative nanosilica mediated approach against fungal biodeterioration of concrete materials. Case Studies in Construction Materials, 17, p.e01258.

Biswas, Jayant, et al. "Biodeterioration agents: Bacterial and fungal diversity dwelling in or on the pre-historic rock-paints of Kabra-pahad, India." *Iranian Journalof Microbiology* 5.3 (2013): 309.

Brehm, Ulrike, Anna Gorbushina, and Derek Mottershead. "The role of microorganisms and biofilms in the breakdown and dissolution of quartz and glass."*Geobiology: Objectives, Concepts, Perspectives*. Elsevier, 2005. 117-12.

Cappitelli, Francesca, et al. "Synthetic consolidants attacked by melanin-producing fungi: Case study of the biodeterioration of Milan (Italy) Cathedral marble treated with acrylics." *Applied and environmental microbiology* 73.1 (2007): 271-277.

Chaudhuri, A., Bhattacharyya, S., Chaudhuri, P., Sudarshan, M. and Mukherjee, S., 2020. In vitro deterioration study of concrete and marble by Aspergillus tamarii. Journal of Building Engineering, 32, p.101774.

Derrick, M. R., Stulik, D., & Landry, J. M. (2000). *Infrared spectroscopy in conservation science*. Getty Publications.

Falchi, L., Balliana, E., Izzo, F. C., Agostinetto, L., & Zendri, E. (2013). Distribution of nanosilica dispersions in Lecce stone. *Sciences at Ca'Foscari*, (1| 2013).

Farrukh, M. A. "Antibacterial and Antifungal Activities of Zinc-Sil-icon Oxides Nanocomposite.(2016) Lett Health Biol Sci 1 (1): 1-5." *Lett Health Biol Sci* 1.1

Fomina, M., Hillier, S., Charnock, J. M., Melville, K., Alexander, I. J., & Gadd, G.

Fomina, M., Podgorsky, V. S., Olishevska, S. V., Kadoshnikov, V. M., Pisanska, I. R., Hillier, S., & Gadd, G. M. (2007). Fungal deterioration of barrier concrete used in nuclear waste disposal. *Geomicrobiology Journal*, *24*(7-8), 643-653.

Gesoglu, M., Güneyisi, E., Öz, H. Ö., Yasemin, M. T., & Taha, I. (2015). Durability and shrinkage characteristics of self-compacting concretes containing recycled coarse and/or fine aggregates. *Advances in Materials Science and Engineering*, *2015*.

Givi, A. N., Rashid, S. A., Aziz, F. N. A., & Salleh, M. A. M. (2011). The effects of lime solution on the properties of SiO_2 nanoparticles binary blended concrete. *Composites Part B: Engineering*, *42*(3), 562-569.

Givi, A.N., Rashid, S.A., Aziz, F.N.A. and Salleh, M.A.M., 2011. Investigations on the development of the permeability properties of binary blended concrete with nano-SiO2 particles. Journal of Composite Materials, 45(19), pp.1931-1938.

Gorbushina, Anna A., and Wolfgang E. Krumbein. "Rock dwelling fungal communities: diversity of life styles and colony structure." *Journey to diverse microbial worlds*. Springer, Dordrecht, 2000. 317-334.

Grayston, S. J., & Wainwright, M. (1987). Fungal sulphur oxidation: effect of carbonsource and growth stimulation by thiosulphate. *Transactions of the British Mycological Society*, *88*(2), 213-219.

Gu, J. D., Ford, T. E., Berke, N. S., & Mitchell, R. (1998). Biodeterioration of concrete by the fungus Fusarium. *International biodeterioration & biodegradation*, *41*(2), 101-109.

Gu, J.D., Ford, T.E., Berke, N.S. and Mitchell, R., 1998. Biodeterioration of concrete by the

fungus Fusarium. International biodeterioration & biodegradation, 41(2), pp.101-109.

Harbulakova, V. O., Estokova, A., Stevulova, N., Luptáková, A., & Foraiova, K. (2013). Current trends in investigation of concrete biodeterioration. *Procedia Engineering*, *65*, 346-351.

Harilal, Manu,et al. "Fungal resistance of nano modifiers and corrosion inhibitor amended fly ash concrete." International Biodeterioration & Biodegradation 143 (2019): 104725.

Herrera, Liz Karen, et al. "Biodeterioration of peridotite and other constructional materials in a building of the Colombian cultural heritage." *International biodeterioration & biodegradation* 54.2-3 (2004): 135-141.

Illescas, Juan F., and Maria J. Mosquera. "Producing surfactant-synthesized nanomaterials in situ on a building substrate, without volatile organic compounds." *ACS applied materials & interfaces* 4.8 (2012): 4259-4269.

Ji, T. (2005). Preliminary study on the water permeability and microstructure of concrete incorporating nano-SiO_2. *Cement and concrete Research*, *35*(10), 1943- 1947.

Ji, T., 2005. Preliminary study on the water permeability and microstructure of concrete incorporating nano-SiO2. Cement and concrete Research, 35(10), pp.1943-1947.

Jiang, J., Zheng, Q., Hou, D., Yan, Y., Chen, H., She, W., ... & Sun, W. (2018). Calcite crystallization in the cement system: morphological diversity, growth

Jurkić, L.M., Cepanec, I., Pavelić, S.K. and Pavelić, K., 2013. Biological and therapeutic effects of ortho-silicic acid and some ortho-silicic acid-releasing compounds: New perspectives for therapy. Nutrition & metabolism, 10, pp.1-12.

Lavigne, M.P., Bertron, A., Auer, L., Hernandez-Raquet, G., Foussard, J.N., Escadeillas, G., Cockx, A. and Paul, E., 2015. An innovative approach to reproduce the biodeterioration of industrial cementitious products in a sewer environment. Part I: Test design. Cement and Concrete Research, 73, pp.246-256.

Li, H., Xiao, H. G., Yuan, J., & Ou, J. (2004). Microstructure of cement mortar with nano-particles. *Composites Part B: Engineering*, *35*(2), 185-189.

Luo, J., Chen, X., Crump, J., Zhou, H., Davies, D. G., Zhou, G., ... & Jin, C. (2018). Interactions of fungi with concrete: Significant importance for bio-based self-healing concrete. *Construction and Building Materials*, *164*, 275-285.

M. (2005). Role of oxalic acid overexcretion in transformations of toxic metal minerals by

Beauveria caledonica. *Appl. Environ. Microbiol.*, *71*(1), 371-381.

Marshman, N. A., & Marshall, K. C. (1981). Bacterial growth on proteins in the presence of clay minerals. *Soil Biology and Biochemistry*, *13*(2), 127-134.

mechanism and shape evolution. *Physical Chemistry Chemical Physics*, *20*(20), 14174-14181.

Ogihara, Hitoshi, et al. "Simple method for preparing superhydrophobic paper: spray-deposited hydrophobic silica nanoparticle coatings exhibit high water-repellency and transparency." *Langmuir* 28.10 (2012): 4605-4608.

Pan, X., Shi, Z., Shi, C., Ling, T. C., & Li, N. (2017). A review on concrete surface treatment Part I: Types and mechanisms. *Construction and Building Materials*, *132*,578-590.

Rosado, Tânia, et al. "Microorganisms and the integrated conservation-intervention process of the renaissance mural paintings from Casas Pintadas in Évora–Know to act, act to preserve." *Journal of King Saud University-Science* 29.4 (2017): 478-486.

Sanchez-Silva, M., & Rosowsky, D. V. (2008). Biodeterioration of construction materials: state of the art and future challenges. *Journal of Materials in Civil Engineering*, *20*(5), 352-365.

Scevola, D., et al. "Antibacterial activity of nanomolecular silicon dioxide (sio2) combined with silver iones." *Clinical Microbiology & Infection* 18 (2012): 389-390.

Tiano, P. (2002, April). Biodegradation of cultural heritage: decay mechanisms and control methods. In *Seminar article, New University of Lisbon, Department of Conservation and Restoration* (pp. 7-12).

Tiano, P., 2002, April. Biodegradation of cultural heritage: decay mechanisms and control methods. In Seminar article, new university of Lisbon, Department of Conservation and Restoration (pp. 7-12).

Verrecchia, Eric P. "Fungi and sediments." *Microbial sediments*. Springer, Berlin, Heidelberg, 2000. 68-75.

Vishwakarma, Vinita, R. P. George, D. Ramachandran, B. Anandkumar, and U. Kamachi Mudali. "Studies of detailed Biofilm characterization on fly ash concrete in comparison with normal and superplasticizer concrete in seawater environments." Environmental technology 35, no. 1 (2014): 42-51.

Wainwright, M., Al-Wajeeh, K. and Grayston, S.J., 1997. Effect of silicic acid and other silicon compounds on fungal growth in oligotrophic and nutrient-rich media. Mycological Research, 101(8), pp.933-938.